AECL EACL

CA0900542

AECL-12100

Surface Chemistry Interventions to Control Boiler Tube Fouling - Part II

Interventions en chimie de surface pour contrôler l'encrassement des tubes de générateurs de vapeur – Partie II

C.W. Turners, D.A. Guzonas*, and S.J. Klimas

June 2004 Juin

AECL

SURFACE CHEMISTRY INTERVENTIONS TO CONTROL BOILER TUBE FOULING - PART II

by

C.W. Turner, D.A. Guzonas*, and S.J. Klimas.

Reactor Chemistry Branch* and Component Life Technology Branch
Atomic Energy of Canada Limited
Chalk River Laboratories,
Chalk River, Ontario K0J 1J0

2004 June

AECL-12100

AECL

SURFACE CHEMISTRY INTERVENTIONS TO CONTROL BOILER TUBE FOULING - PART II

by

C.W. Turner, D.A. Guzonas*, and S.J. Klimas

PREFACE

This is the third in a series of reports from an investigation co-funded by the Electric Power Research Institute (EPRI) and by Atomic Energy of Canada Limited (AECL) into the effectiveness of alternative amines for controlling the rate of tube-bundle fouling under steam generator (SG) operating conditions. The objectives of this investigation are to determine whether the fouling rate depends on the amine used for pH control, to identify those factors that influence the effectiveness, and use this information to optimize the selection of an amine for chemistry control and deposit control in the steam cycle and steam generator, respectively. Work to date has demonstrated that the rate of particle deposition under steam generator operating conditions is strongly influenced by surface chemistry (Turner et al., 1997; Turner et al., 1999). This dependence upon surface chemistry is illustrated by the difference between the deposition rates measured for hematite and magnetite, and by the dependence of the particle deposition rate on the amine used for pH control.

Deposition rates of hematite were found to be more than 10 times greater than those for magnetite under similar test conditions (Turner et al., 1997). At 270°C and $pH_T = 6.2$, the surfaces of hematite and magnetite are predicted to be positively charged and negatively charged, respectively (Shoonen, 1994). Measurements of the point of zero charge (PZC) of magnetite at temperatures from 25°C to 290°C by Wesolowski et al. (1999) have confirmed that magnetite is negatively charged at the stated conditions. A PZC of 4.2 was measured for Alloy 600 at 25°C (Balakrishnan and Turner, un-published results), and its surface is expected to remain negatively

Reactor Chemistry Branch* and Component Life Technology Branch
Atomic Energy of Canada Limited
Chalk River Laboratories,
Chalk River, Ontario K0J 1J0

2004 June

AECL-12100

charged for alkaline chemistry over the temperature range of interest. Therefore, there will be a repulsive force between the surfaces of magnetite particles and Alloy 600 at 270°C and $pH_T = 6.2$ that is absent for hematite particles depositing under the same conditions. This difference is consistent with the higher deposition rates found for hematite particles on Alloy 600. The deposition rate of hematite was also found to be sensitive to the redox conditions in the test loop (Turner et al., 1999). Thus, the highest deposition rates were measured when there was a residual of dissolved oxygen in the loop water and no hydrazine, whereas the deposition rates tended to decrease towards those of magnetite in tests with residual hydrazine and little or no dissolved oxygen. This result, again, points to the importance of surface charge in governing the rate of particle deposition.

The dependence of the particle deposition rate on the amine used for pH control was postulated to be associated with differences in the degree of adsorption of amine onto the surface of the magnetite particles and the associated effect this would have on surface charge. Amine molecules exist in solution as both the neutral, A, and hydrolysed, HA^+, species. Adsorption of the latter was postulated to make the surface of magnetite less negative and, consequently, to reduce the force of repulsion between the magnetite particles and Alloy 600. Subsequent measurements at 25°C showed that the amine molecules did adsorb onto magnetite to varying degrees, and that this adsorption was associated with a decrease in the force of repulsion between the surfaces of magnetite and Alloy 600 (Turner et al., 1999). There also appeared to be a correlation between the amount of amine adsorbed at 25°C and the deposition rate measured at 270°C. The reduction in surface charge deduced from the force measurements was small, however, compared to the amount of amine adsorbed. Also, both the adsorption and the base strength of the amines decrease with increasing temperature which makes the connection between adsorption measurements at 25°C and deposition behaviour at 270°C less certain. Doubt as to the validity of the hypothesis was also cast by the results of Wesolowski et al. (1999) and Bénézeth et al. (2000) who found no effect of the adsorption of amine on the high-temperature surface charge properties of magnetite.

Results from further experiments to determine the mechanism by which amines affect the rate of tube-bundle fouling and, thus, facilitate optimization of the amine used for pH control in the steam cycle and deposit control in the steam generator are reported here. The hypothesis that the amine affects the deposition rate through a surface-charge effect was tested by measuring the deposition rate of magnetite as a function of amine concentration in buffered solutions at constant pH_T. Measurements of the kinetics of adsorption and desorption of amine as a function of temperature were also conducted to help relate the surface chemistry at 25°C with deposition behaviour measured at 270°C. Finally, the relationship between hydrophobicity and the particle deposition rate was investigated further by measuring the effect of amine on the wetting angle at temperatures up to 220°C (the practical limit of the apparatus).

Reactor Chemistry Branch* and Component Life Technology Branch
Atomic Energy of Canada Limited
Chalk River Laboratories,
Chalk River, Ontario K0J 1J0

2004 June

AECL-12100

EACL

INTERVENTIONS EN CHIMIE DE SURFACE POUR CONTRÔLER L'ENCRASSEMENT DES TUBES DE GÉNÉRATEURS DE VAPEUR – PARTIE II

par

C. W. Turner, D. A. Guzonas*, et S. J. Klimas.

Préface

Il s'agit du troisième d'une série de rapports tirés d'une étude financée conjointement par l'Electric Power Research Institute (EPRI) et Énergie atomique du Canada limitée (EACL) et portant sur l'efficacité des amines alternatives pour limiter la vitesse d'encrassement des faisceaux tubulaires dans des conditions de fonctionnement des générateurs de vapeur (GV). La présente étude a pour objectifs de déterminer si la vitesse d'encrassement dépend de l'amine utilisée pour contrôler le pH, de déterminer les facteurs ayant un effet sur l'efficacité et d'utiliser les renseignements obtenus pour optimiser le choix d'une amine en vue du contrôle chimique et du contrôle des dépôts respectivement dans le cycle de production de vapeur et dans le générateur de vapeur. Les travaux ont jusqu'ici permis de démontrer que la chimie de surface influe considérablement sur la vitesse unitaire de dépôt des particules dans les conditions de fonctionnement du générateur de vapeur (Turner et coll., 1997; Turner et coll., 1999). Cette dépendance vis-à-vis de la chimie de surface est illustrée par la différence entre les vitesses de dépôt mesurées pour l'hématite et la magnétite ainsi que par la dépendance de la vitesse de dépôt vis-à-vis des particules sur l'amine utilisée pour le contrôle du pH.

On a observé que les vitesses de dépôt de l'hématite étaient 10 fois plus élevées que celles de la magnétite soumise à des conditions d'essai semblables (Turner et coll., 1997). À 270 C et avec un $pH_T = 6,2$, on prévoit que les surfaces de l'hématite et de la magnétite seront respectivement

Chimie des réacteurs* et Technologie de la durée de vie des composants
Laboratoires de Chalk River
Atomic Energy of Canada Limited
Chalk River Laboratories,
Chalk River, Ontario K0J 1J0

2004 Juin

AECL-12100

de charge positive et négative (Shoonen, 1994). Les mesures au point de charge zéro (PCZ) de la magnétite à des températures allant de 25 à 290°C effectuées par Wesolowski et coll. (1999) ont confirmé que la magnétite est de charge négative dans les conditions données. Un PCZ de 4,2 a été mesuré pour l'alliage 600 à 25 C (Balakrishnan et Turner, résultats non publiés), et l'on prévoit que sa surface demeurera chargée négativement pour la chimie alcaline dépassant la plage de température qui nous intéresse. Il y aura donc une force de répulsion entre les surfaces des particules de magnétite et de l'alliage 600 à 270 C et au $pH_T = 6,2$ qui n'existe pas dans le cas des particules d'hématite qui se déposent dans les mêmes conditions. Cette différence correspond aux vitesses de dépôt plus élevées observées pour les particules d'hématite sur l'alliage 600. On a également observé que la vitesse de dépôt de l'hématite réagissait aux conditions redox dans la boucle d'essai (Turner et coll., 1999). Ainsi, les vitesses de dépôt les plus élevées ont été enregistrées lorsqu'il y avait un résidu d'oxygène dissous dans l'eau de la boucle et absence d'hydrazine, alors que les vitesses de dépôt avaient tendance à diminuer pour se rapprocher de celles des essais de magnétite avec un résidu d'hydrazine et peu ou pas d'oxygène dissous. Une fois encore, ce résultat indique l'importance de la charge de surface sur le contrôle de la vitesse de dépôt des particules.

On a émis l'hypothèse que la dépendance de la vitesse de dépôt des particules sur l'amine utilisée pour le contrôle du pH était associée aux différences dans le degré d'adsorption de l'amine sur la surface des particules de magnétite et l'effet que cela aurait sur la charge de surface. Les molécules d'amine existent en solution à la fois comme espèce neutre A et comme espèce hydrolysée HA^+. On a émis l'hypothèse que l'adsorption de cette dernière rendrait la surface de magnétite moins négative et, par conséquent, qu'elle réduirait la force de répulsion entre les particules de magnétite et l'alliage 600. Des mesures ultérieures à 25°C montrent que les molécules d'amine se sont bel et bien adsorbées sur la magnétite à des degrés variables et que cette adsorption était attribuable à une réduction de la force de répulsion entre les surfaces de magnétite et d'alliage 600 (Turner et coll., 1999). Il semblait également y avoir corrélation entre la quantité d'amine adsorbée à 25 C et la vitesse de dépôt mesurée à 270 C. Cependant, la réduction de la charge de surface déduite des mesures de la force était faible comparativement à la quantité d'amines adsorbées. En outre, l'adsorption et la force de base des amines diminuent avec une hausse de température, ce qui rend moins certain le lien entre les mesures d'adsorption à 25 C et le comportement des dépôts à 270 C. Les résultats de Wesolowski et coll. (1999) et de Bénézeth et coll. (2000) mettent également en doute la validité de l'hypothèse puisqu'ils n'ont trouvé aucun effet de l'adsorption d'amine sur les caractéristiques de la charge de surface de la magnétite à haute température.

Le présent rapport présente un compte-rendu des résultats d'autres expériences visant à déterminer le mécanisme selon lequel les amines influent sur la vitesse d'encrassement des faisceaux tubulaires et facilitent ainsi l'optimisation de l'amine utilisée pour contrôler le pH dans

Chimie des réacteurs* et Technologie de la durée de vie des composants
Laboratoires de Chalk River
Atomic Energy of Canada Limited
Chalk River Laboratories,
Chalk River, Ontario K0J 1J0

2004 Juin

AECL-12100

le cycle de production de vapeur et dans le contrôle des dépôts dans les générateurs de vapeur. On a vérifié l'hypothèse voulant que l'amine influe sur la vitesse de dépôt par un effet de charge de surface en mesurant la vitesse de dépôt de la magnétite comme facteur de concentration de l'amine dans des solutions tampons à un pH_T constant. On a également effectué des mesures de la cinétique de l'adsorption et de la désorption de l'amine comme facteur de la température afin d'aider à établir le lien entre la chimie de surface à 25 C et le comportement des dépôts mesuré à 270 C. Enfin, on a étudié de plus près le rapport entre l'hydrophobicité et la vitesse de dépôt des particules en mesurant l'effet de l'amine sur l'angle de mouillabilité à des températures s'élevant jusqu'à 220 C (la capacité pratique des appareils).

Chimie des réacteurs* et Technologie de la durée de vie des composants
Laboratoires de Chalk River
Atomic Energy of Canada Limited
Chalk River Laboratories,
Chalk River, Ontario K0J 1J0

2004 Juin

AECL-12100

TABLE OF CONTENTS

TABLES

TABLE OF CONTENTS

SECTION **PAGE**

FIGURES

TABLE OF CONTENTS

SECTION **PAGE**

TABLE OF CONTENTS

SECTION **PAGE**

APPENDICES

1. EXPERIMENTAL METHODS AND ANALYSES

1.1 Adsorption Isotherms

The adsorption of dimethylamine (DMA) and morpholine onto the surface of magnetite particles with specific surface area equal to 3.98 m^2/g was measured using a solution depletion method. The concentration of amine in the solution contacting a known quantity of magnetite particles was measured using Laser Raman Spectroscopy. Details of the experimental procedure are similar to those reported previously (Turner et al., 1999). This time, however, spectra were measured as a function of time following the addition of magnetite to the solution to measure the adsorption kinetics at 25°C. Once equilibrium between the solution and particles had been achieved at 25°C, the samples were heated in a high-temperature Raman cell and held at selected temperatures to measure the rate of desorption of the amine from the surface of the particles. For the desorption measurements, spectra were collected at temperature intervals of approximately 20°C. Heating time to reach the target temperature ± 5°C was typically 5 min. Once thermal stability was attained (after an additional 5 min) Raman spectra were collected at the rate of 1 every 2-3 min.

Raman intensities were converted to amine concentrations using the calibration curve measured previously (Turner et al., 1999). Potassium perchlorate was added to the solutions as an internal standard to normalize the spectra collected at different temperatures and to account for differences in signal intensity associated with sample positioning, laser power, and data acquisition time. Perchlorate ion was used for this application because it is a non-complexing ion and is not expected to adsorb onto the surface of magnetite to a significant extent. Details of how the quantity of amine adsorbed was calculated from the normalized Raman intensities is described in Appendix A of this report.

The spectral region of the perchlorate ion symmetric stretch measured for morpholine and DMA solutions containing the perchlorate internal standard is shown in Figure 1-1. In addition to the perchlorate band at 938 cm^{-1}, the spectrum of the morpholine solution contains a strong morpholine band at 831 cm^{-1}, and a number of weaker morpholine bands between 1000-1350 cm^{-1} which are superimposed on the broad silica Raman band from the cell window. The spectrum of the DMA solution is much simpler, containing only a weak band at 895 cm^{-1} from DMA in addition to the perchlorate band at 938 cm^{-1}.

The band areas of the perchlorate band at 938 cm^{-1} from both the morpholine and DMA experiments are plotted as a function of temperature in Figure 1-2. The band areas in the DMA experiment are essentially constant at all temperatures, while the band areas increase with temperature in the morpholine experiment. Since the temperature axis is also a time axis (the temperatures were measured in sequence from low to high with roughly the same interval between each temperature), this suggests a slow drift in alignment or laser power throughout the morpholine experiment. This change in instrument parameters is removed by scaling all the intensities to the intensity at room temperature, as discussed in Appendix A of this report.

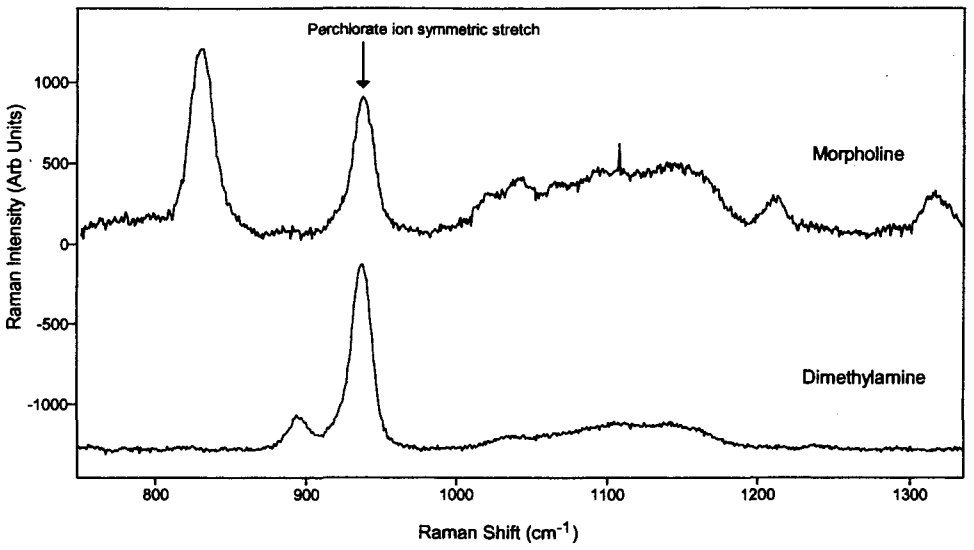

Figure 1-1: Raman spectra of the perchlorate ion symmetric stretching region of morpholine and DMA solutions containing potassium perchlorate at room temperature.

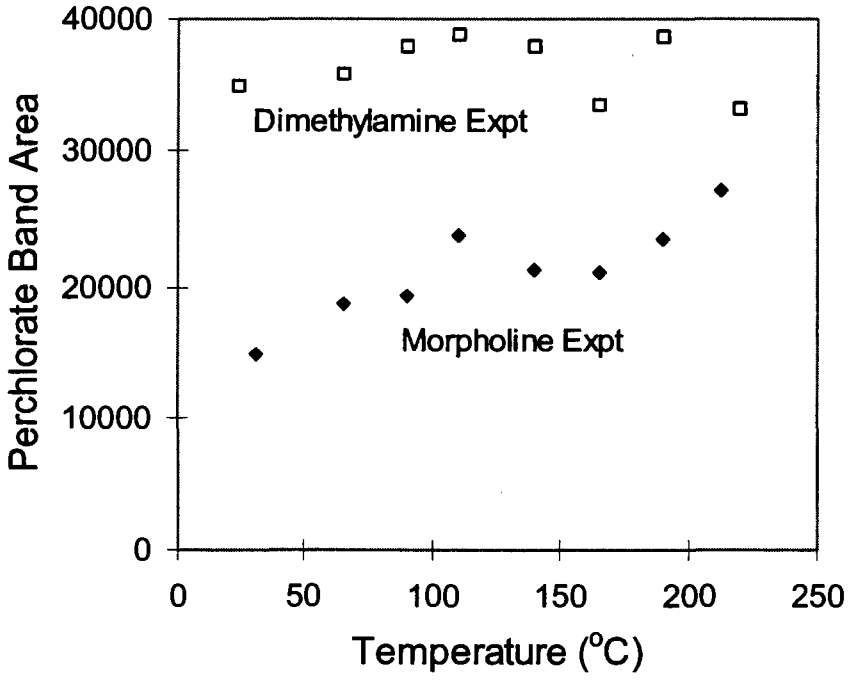

Figure 1-2: Band area of the perchlorate ion symmetric stretching mode at 938 cm^{-1} as a function of temperature for adsorption measurements with morpholine and DMA.

1.2 Atomic Force Microscopy

The same procedures reported previously to measure the interaction force between surfaces of magnetite and Alloy 600 (Turner et al., 1999) were used to investigate the kinetics of the adsorption and desorption of DMA and morpholine at 25°C. Coupons of Alloy 600 were polished to a 0.06 μm finish using alumina, and then autoclaved at pH 9 with morpholine at a temperature of 250°C to grow a corrosion film. The average surface roughness of the Alloy 600 substrate after exposure in the autoclave was ~25 nm. The same coupon was used throughout the entire series of experiments. Between each experiment, the surface was lightly polished with 0.06 μm alumina and cleaned with methanol in an ultrasonic bath for a period of 30 min. A fresh particle of magnetite was used for each experiment.

Initial measurements of the force curve versus pH in amine-free water were used to determine the point of zero charge (PZC) of each particle/surface combination. Any particle/surface combination that exhibited anomalous behaviour was excluded from further measurements. Anomalous behaviour is typically a result of one of the following factors: contamination of one or the other surface so that it does not develop a pH-dependent surface charge, contamination of the suspension by a dust particle that interferes with the magnetite/Alloy 600 interaction potential, or a piece of the magnetite particle falling off and sticking to the Alloy 600 surface.

The kinetics of both the adsorption and desorption of amine were investigated by measuring force curves as a function of time. Measurements were made at $pH_{25} \approx 7$, i.e., just above the PZC of magnetite, and at pH_{25} 10. The solution pH was adjusted with mixtures of potassium hydroxide and perchloric acid so that pH would be independent of the concentration of amine. To measure the adsorption kinetics, force curve data were acquired as rapidly as possible (roughly 30 s between force curve measurements) during the initial 30 min following the addition of a 50 mg/kg solution of amine to the measurement cell. After an interval of 30 min, the frequency at which force curves were measured was reduced to one every 5 to 10 min. Once a steady-state had been attained, the desorption kinetics were measured by flushing the cell with amine-free water at the same pH and ionic strength as used for the adsorption measurements and measuring the force curve as a function of time in the same manner as described above.

Although precautions were taken to ensure that both the apparatus and the solutions were at thermal equilibrium with the ambient room temperature before the start of data acquisition, data measured during the first 10 min of filling the sample cell may be affected by thermal drift.

1.3 Surface Contact Angle

The cell used for the Raman measurements at elevated temperatures was found to be suitable for measuring the temperature dependence of the contact angle of aqueous solutions of amine on solid surfaces. Contact angles for 50 mg/kg solutions of DMA and morpholine at the surfaces of Alloy 600 and a single crystal of magnetite were measured over the temperature range 25-190°C using the same experimental procedures that were reported previously (Turner et al., 1999). The contact angles were measured from a projection of the meniscus onto a vertical surface behind the cell. For the DMA experiment, the contact angles were also measured on photographs of the cell. Obtaining an image of the meniscus by projection onto a vertical surface is simpler and

cheaper than by photography; the latter being more labour intensive and, therefore, more expensive. The quality of the photographs is quite high, whereas the projected image appeared to be disturbed by convection currents at elevated temperatures. Thus, the results from measurements of contact angle on the photographs are considered to be more reliable than those on the projected image.

1.4 Loop Fouling Tests

Measurements of the effect of the concentration of DMA and morpholine on the fouling rate of magnetite particles under flow-boiling conditions were made using the same methods and loop conditions as described previously (Turner et al., 1999). A suspension of colloidal magnetite particles radiotraced with 59-Fe is injected continuously from a carboy into the loop during each test and the rate of build-up of deposit monitored on the test section using an on-line gamma detector. At the end of each run, the test section is removed and the deposit distribution measured along the length of the test section using an off-line gamma detector system. This information is used to calculate a normalized fouling rate as a function of thermodynamic mixture quality. Nominal loop conditions used in this investigation are listed in Table 1-1. Details for individual tests are listed in Table B-1.

Table 1-1: Nominal Loop Test Conditions

Pressure MPa	Heat Flux kW/m^2	Mass Flux $kg/m^2 \cdot s$	$T_{saturation}$ °C	Quality
5.6	230	300	270	-0.28 - +0.55

Tests were performed with magnetite equilibrated with two different concentrations of amine to investigate the effect of amine concentration on the particle fouling rate. Buffered solutions were prepared by mixing the amine of interest with a known amount of strong acid to ensure that each test was done at $pH_T = 6.2$ (at a temperature of 270°C) regardless of the concentration of amine. Hydrochloric acid was selected to prepare the buffer solution in 6 of the loop tests because it is a non-oxidizing, non-complexing acid. For 2 of the loop tests, hydrochloric acid was replaced with triflouromethanesulphonic ("triflic") acid. Both are strong acids and were assumed to be fully dissociated at all temperatures. The concentrations of acid and amine used to prepare the buffer solutions are listed in Table 1-2.

Table 1-2: Composition of Buffer Solution to Control pH for Loop Fouling Tests.

Amine		Acid		pH	
				25°C	270°C
Morpholine	5 mM	HCl or "triflic"	0.32 mM	9.6	6.2
Morpholine	50 mM	HCl or "triflic"	3.2 mM	9.7	6.2
DMA	5 mM	HCl or "triflic"	3.3	10.8	6.2
DMA	50 mM	HCl or "triflic"	33	11.0	6.2

A total of 8 loop tests were performed. In all of these tests the magnetite suspension in the carboy was equilibrated with the buffered solution of amine (with a concentration of either 5 mM or 50 mM, as indicated in Table 1-2) prior to being injected into the loop. In the first 5 tests in the series the loop chemistry was controlled using the same buffered amine solution as used in the carboy. However, the high concentration of acid required to buffer the 50 mM solution of DMA caused corrosion to occur in one of the valves on the loop that happened to be leaking at the valve stem. Although the valve was replaced, in subsequent tests the high concentration of amine was used in the carboy only and the loop chemistry was controlled using amine at a sufficient concentration to maintain $pH_{270} = 6.2$. Specific chemistry conditions for each test are listed in Tables 1-3 and B-1.

Table 1-3: Chemistry Conditions for the Loop Fouling Tests

Test	Amine	Acid	Amine Concentration (mM)		O_2 (µg/kg)	N_2H_4 (µg/kg)
			Loop	Carboy		
D-136	morpholine	HCl	5	5	< 5	200
D-137	morpholine	HCl	50	50	< 5	75
D-138	DMA	HCl	5	5	< 5	20
D-139	DMA	HCl	50	50	35	110
D-144	morpholine	trifilic	5	5	< 5	70
D-145	morpholine	trifilic	0.20	50	< 5	100
D-146	morpholine	HCl	0.23	50	< 5	50
D-147	DMA	HCl	0.040	50	< 5	80

Prior to conducting the 8 loop tests, 2 additional on-line gamma ray detectors were installed on the loop. Under the test conditions, the 3 on-line gamma detectors monitor the build-up of deposit on the test section at thermodynamic mixture qualities of approximately -0.20, +0.20 and +0.40. These same detectors were used to measure the rate of deposit removal using the following procedure. After monitoring deposit build-up for a period of up to 50 h, the magnetite injection pump is switched off and the loop operated for a further 20 h or so while continuing to monitor deposit activity with the on-line gamma detectors. Since the source term for deposition has been removed, i.e., the injection of magnetite into the loop has ceased, during this stage of the loop test the on-line gamma detectors measure the rate at which deposit is being removed from the test section.

The rate of removal of deposit is generally assumed to be proportional to the deposit mass (Epstein, 1988). Thus, once injection of magnetite into the loop has ceased, the deposit mass should decrease exponentially with a removal time-constant λ_r :

$$m(t) = m(t_o) \cdot \exp(-\lambda_r \cdot t) \qquad (1)$$

Beal et al. (1986) elaborated on this concept by noting that for a multi-layered deposit only the outer layer of deposit is subject to removal, and therefore the deposit mass in Equation (1) should be the mass of the outer layer of deposit at the deposit/fluid interface.

In a further elaboration, it has been postulated that the outer layer of deposit is subject to a second process, acting in parallel with removal, called "consolidation" (Turner and Klimas, 2001). The driving force for consolidation is precipitation of dissolved species within the pores of the deposit. The proposed mechanisms of consolidation include Ostwald ripening, dissolution and re-precipitation of deposit in a temperature gradient, and boiling-induced precipitation of dissolved species present in the water. Consolidation results in an increase in both the strength and density of the deposit as a function of time. It is further postulated that the consolidated portion of the deposit is not subject to removal.

A complete discussion of how consolidation affects the fouling kinetics (including both the initial rate of deposit build-up and the rate of removal) is outside of the scope of this investigation. A new fouling model that includes the effect of consolidation has been described in detail elsewhere (Turner and Klimas, 2001). The effect of consolidation on the rate of deposit removal as predicted by the model for the removal phase of a loop test is summarized below.

In the absence of consolidation, the entire deposit mass will be subject to removal. Thus, during the removal phase of a fouling test, i.e., after switching off the magnetite injection pump, the deposit mass should decrease exponentially to zero with a time constant of λ_r, according to Equation (1). In the presence of consolidation, however, only a fraction of the total deposit mass will remain un-consolidated at the end of the deposition phase of the test. During the removal phase, the model predicts that the mass of un-consolidated deposit will decrease exponentially to zero with a time constant equal to the sum $\lambda_r + \lambda_c$, leaving behind a mass of consolidated deposit on the test section. Thus, we can distinguish two cases:

No consolidation: $m(t) \rightarrow 0$ as $t \rightarrow \infty$ during removal, and,

With consolidation: $m(t) \rightarrow m_{consolidated} (\neq 0)$ as $t \rightarrow \infty$ during removal,

where m(t) is equal to the total deposit mass, i.e., consolidated + un-consolidated deposit.

2. RESULTS

2.1 Adsorption and Desorption of Amine

2.1.1 Adsorption Kinetics at 25°C

Figure 2-1 shows the Raman spectra of DMA and morpholine at 25°C in the CH stretching region. The spectra have been baseline corrected to remove the large sloping background from the OH stretch of water. Both amines have strong bands near 2975 cm^{-1} that were used to quantify the quantity of amine that was adsorbed. The frequencies of these bands showed only a slight variation with temperature.

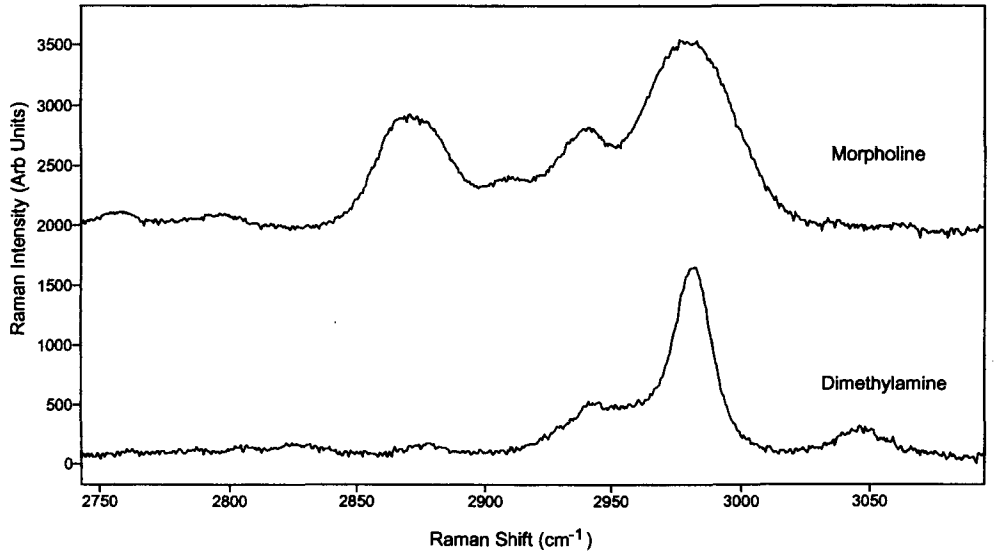

Figure 2-1: Raman spectra of the CH stretching region of 200 mM solutions of DMA and morpholine at 25°C.

The time dependence of the adsorption of morpholine and DMA from 200 mM solutions of the amines onto magnetite at 25°C is shown in Figures 2-2 and 2-3, respectively. Both amines adsorbed relatively slowly at 25°C, with DMA taking approximately twice as long as morpholine to reach a steady-state. Attempts were also made to monitor the desorption of amine by replacing the amine solution in contact with the magnetite with amine-free water at the same pH, but the concentration of desorbed amine was too low to give conclusive results.

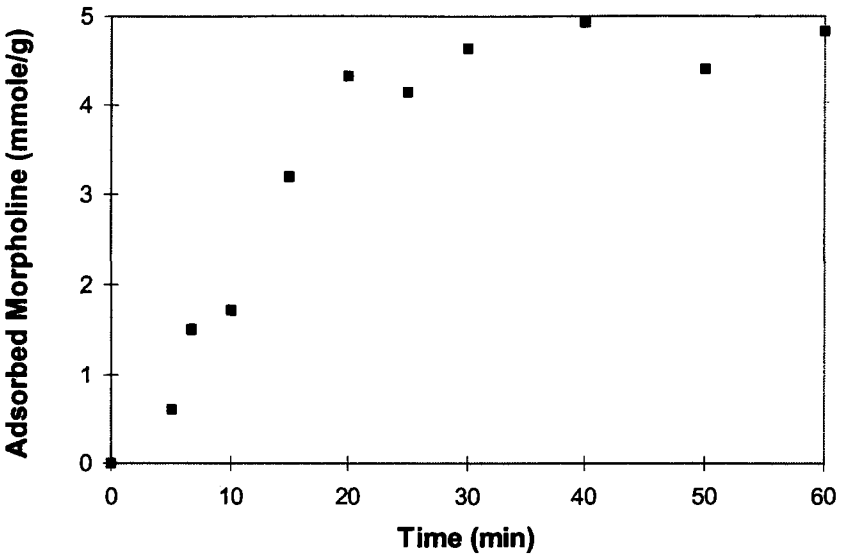

Figure 2-2: Concentration (mM of amine/g magnetite) of morpholine adsorbed onto magnetite as a function of exposure time to a 200 mM solution of morpholine at 25°C.

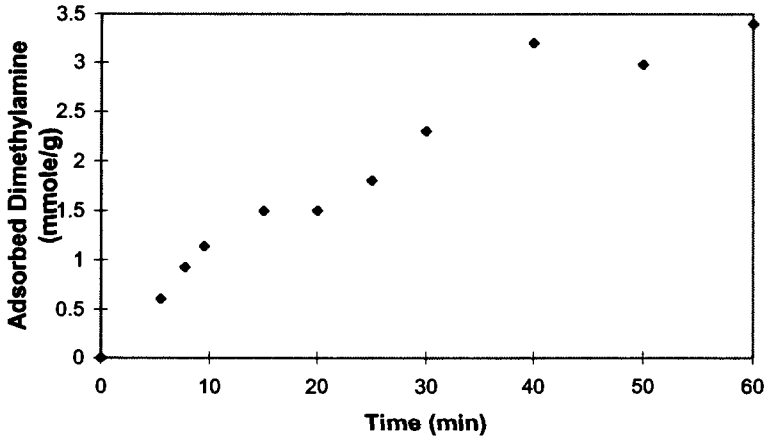

Figure 2-3: Concentration (mM of amine/g magnetite) of DMA adsorbed onto magnetite as a function of exposure time to a 200 mM solution of DMA at 25°C.

2.1.2 Desorption Kinetics at Elevated Temperature

The band areas of the strongest CH stretching band of DMA and morpholine, normalized to the perchlorate band intensities, are plotted in Figure 2-4 as a function of temperature. Some of the variation in band intensity may be an artifact of the curve-fitting routine used to determine the band intensities. Curve fitting to the DMA data required the addition of an extra band in the methanol region for temperature > 140°C, which suggests that some thermal decomposition of DMA has occurred at elevated temperature.

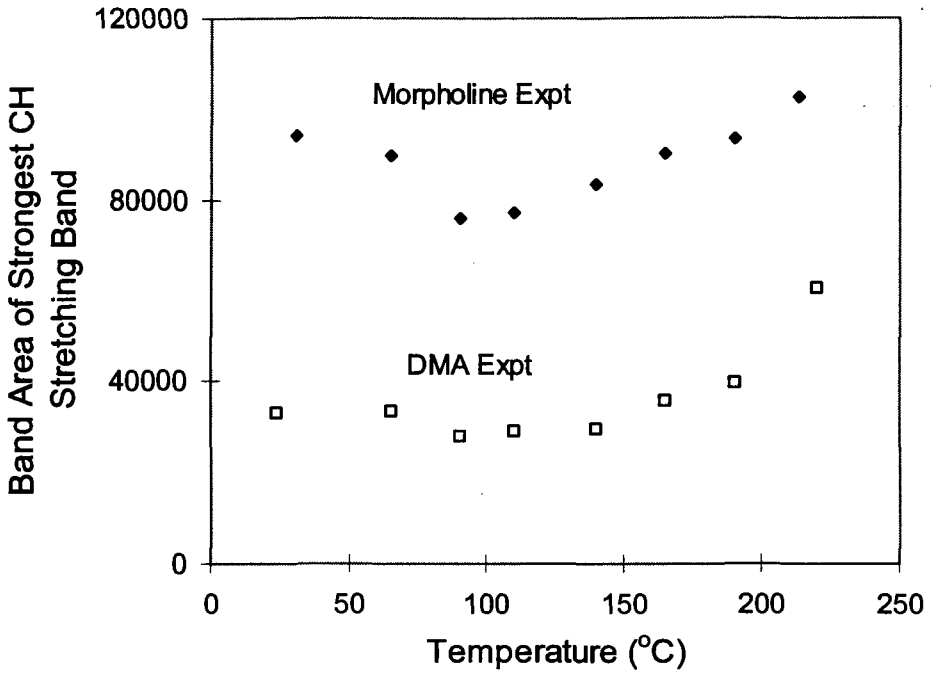

Figure 2-4: Band area of the morpholine and DMA CH stretching bands near 2975 cm^{-1} as a function of temperature.

The desorption of morpholine from the surface of magnetite particles is shown as a function of time and temperature in Figure 2-5. The figure shows that morpholine desorbs from the surface of magnetite for temperatures ≥ 90°C. In addition, much of the desorption takes place within the time taken to heat the sample to the temperature of interest, i.e., before the t = 0 spectra was collected once thermal stability had been achieved. With the exception of the data measured at 90°C, relatively little additional morpholine is desorbed during the time that the sample is held at temperature.

The concentration of morpholine adsorbed onto the surface of the magnetite particles, as determined from the spectra collected at time t = 0, is shown plotted as a function of temperature in Figure 2-6. This figure shows that the onset of morpholine desorption occurs at a temperature between 90 and 110°C. The adsorbed amount decreases steadily with increasing temperature such that the amount remaining on the surface at a temperature of 187°C is only 19% of what was adsorbed at 25°C.

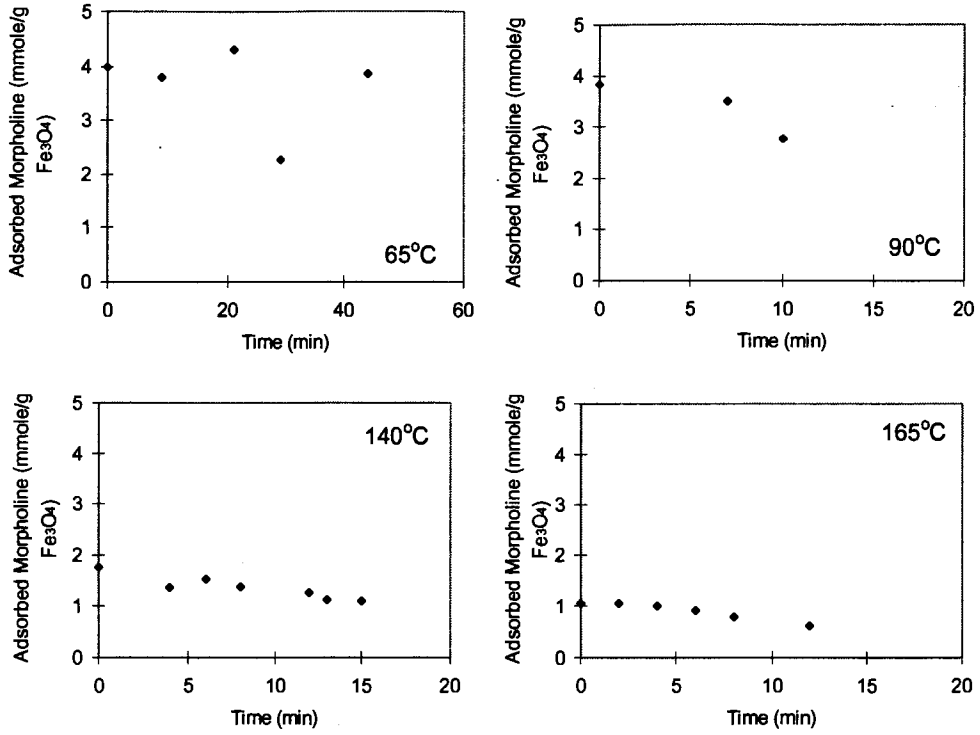

Figure 2-5: Concentration of morpholine (mmole/g magnetite) adsorbed onto magnetite as a function of time and temperature.

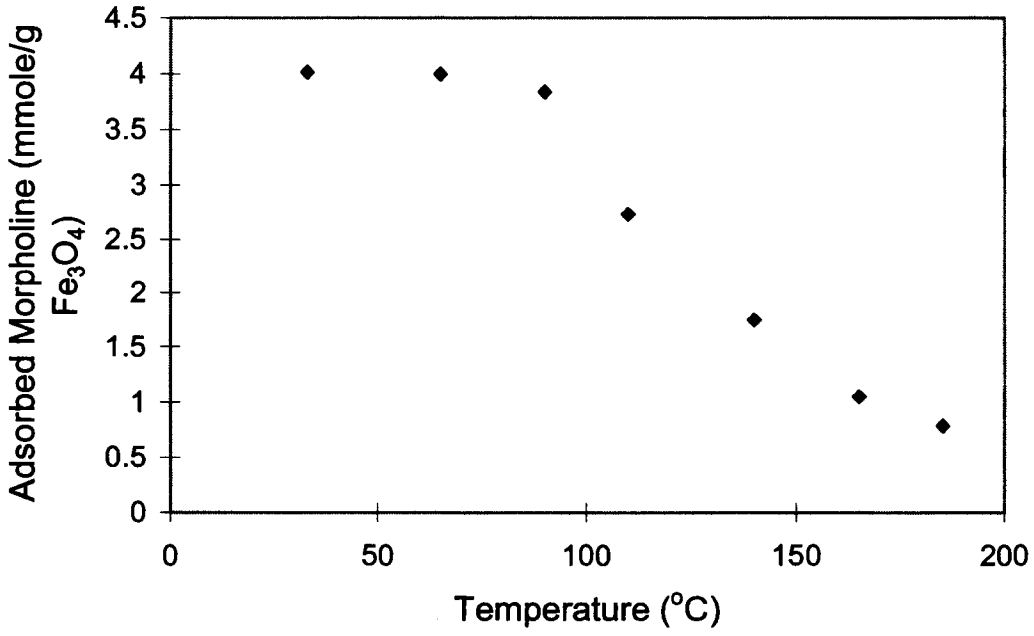

Figure 2-6: Concentration of morpholine (mmole/g magnetite) adsorbed onto magnetite as a function of temperature.

The desorption of DMA from the surface of magnetite particles as a function of time and temperature is shown in Figure 2-7. DMA desorbed much more slowly from the surface of magnetite than morpholine, such that a steady-state was not reached even after holding the sample at the temperature of interest for 15 to 30 min. As a consequence, the concentration of DMA that remained on the surface once thermal equilibrium had been attained, i.e., the amount of adsorbed DMA at t = 0, was significantly higher for DMA than for morpholine. This is illustrated in Figure 2-8, where the adsorbed concentration of DMA measured at t = 0 is shown plotted as a function of temperature. Note that increasing the temperature from 25 to 187°C has only reduced the concentration of adsorbed DMA by 18%. This is to be compared with morpholine where a similar temperature increase reduced the concentration of adsorbed morpholine by over 80%. Although the concentration of adsorbed DMA appears to be significantly lower at a temperature of 220°C (see Figure 2-7), this is a consequence of collecting the spectra at 187°C and 220°C sequentially instead of taking the sample from room temperature to 220°C and then measuring the amount of adsorbed DMA.

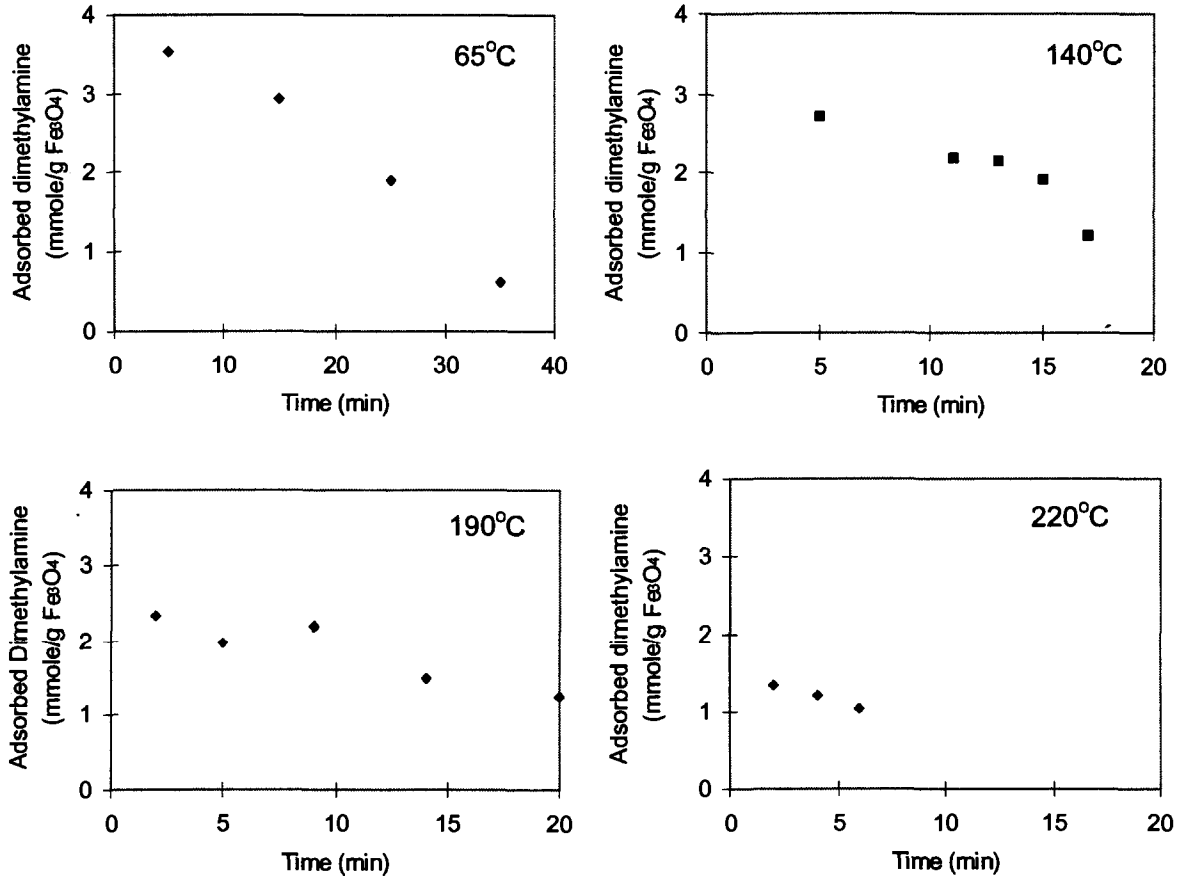

Figure 2-7: Concentration of DMA (mmole/g magnetite) adsorbed onto magnetite as a function of time and temperature.

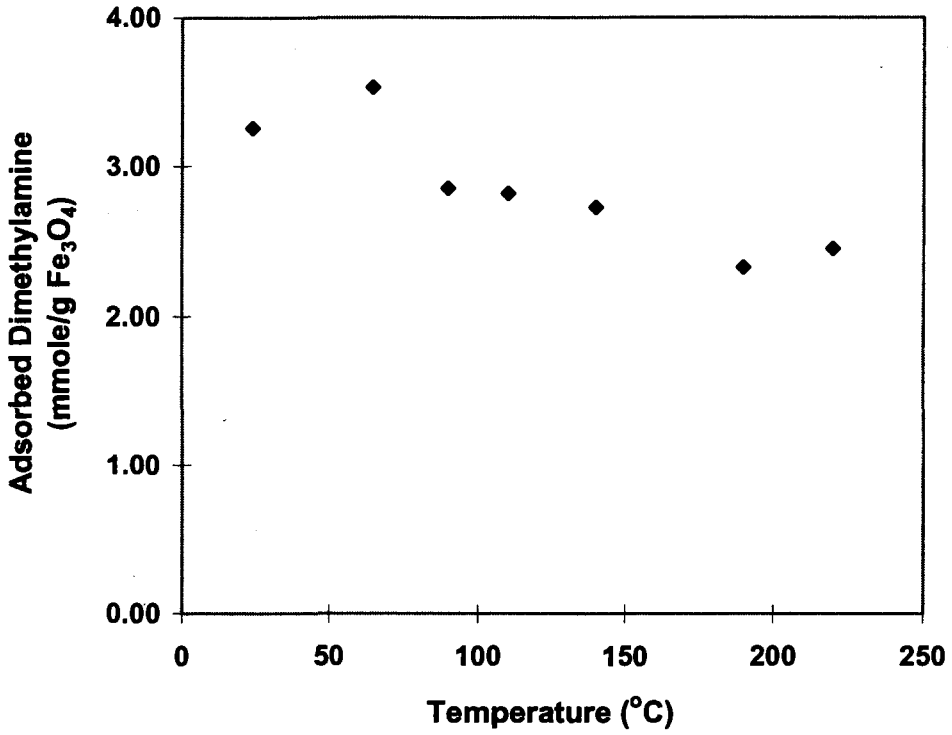

Figure 2-8: Concentration of DMA (mmole/g magnetite) adsorbed onto magnetite as a function of temperature[1].

2.2 Atomic Force Microscopy

2.2.1 Morpholine Adsorption/Desorption Near the PZC of Magnetite

AFM force curves between the surfaces of magnetite and Alloy 600 measured as a function of exposure time to a 50 mg/kg (0.57 mM) solution of morpholine at $pH_{25} = 6.75$ are shown in Figure 2-9. The force measurements are plotted as force per unit particle radius to facilitate comparison with measurements made with particles of different size. Also shown for comparison is the force curve measured in the reference amine-free water at the same pH. In the absence of amine, there is a small force of repulsion between the surfaces of Alloy 600 and magnetite at this pH. With the addition of morpholine, the force becomes more strongly repulsive as a function of exposure time to the amine. Figure 2-10 shows that the force extrapolated to zero separation increases rapidly (by over 600%) during the first 20 min, and thereafter increases by only an additional 39% over the next 40 min. This is the same time scale that was observed for adsorption of morpholine onto the surface of magnetite (see Figure 2-2), which suggests that the increase in the magnitude of the repulsive force is associated with the adsorption of morpholine onto magnetite.

---

[1] Since the 190°C and 220°C samples were run sequentially, the surface concentration at t = 0 for the 220°C sample was corrected for desorption at 190°C.

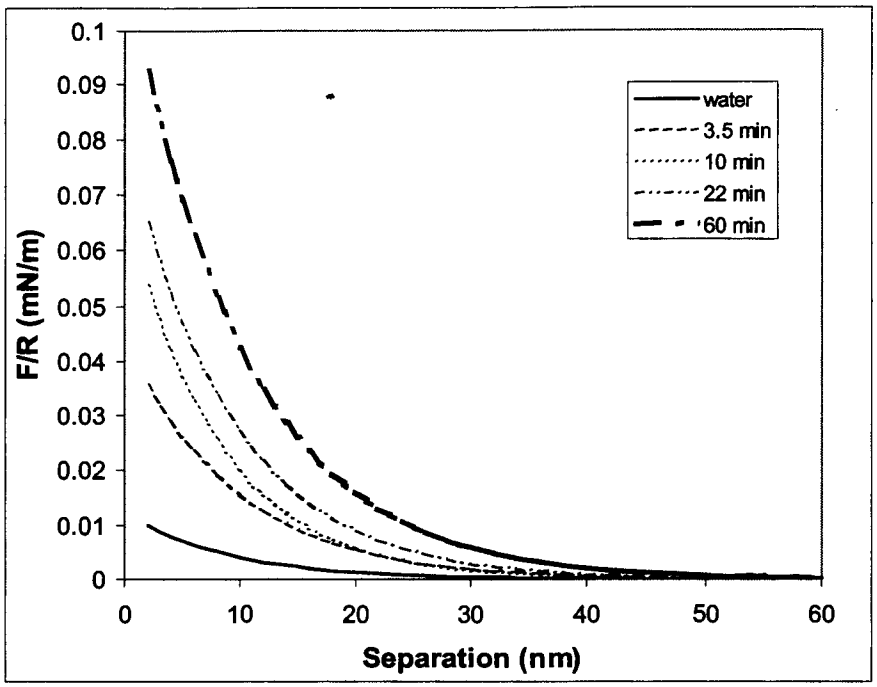

Figure 2-9: **Force between the surface of Alloy 600 and a magnetite particle as a function of separation at selected exposure times to a 50 mg/kg solution of morpholine at pH_{25} 6.75.**

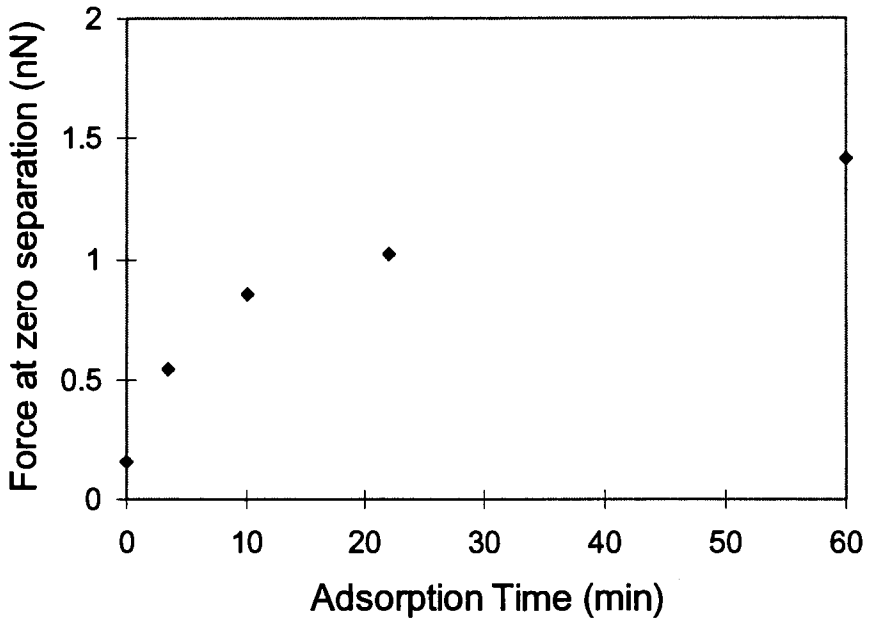

Figure 2-10: **Force between the surface of Alloy 600 and magnetite extrapolated to zero separation as a function of exposure time at pH_{25} 6.75.**

After 1 h of exposure, the morpholine solution was replaced by morpholine-free water at pH_{25} = 6.75. Within 2 min, as shown in Figure 2-11, the force curve was nearly identical to that measured in the reference amine-free water at pH_{25} = 6.75. To the extent that changes in the force curve may be associated with the adsorption and desorption of morpholine, these data indicate that desorption of morpholine from the surface of magnetite is rapid, even at 25°C.

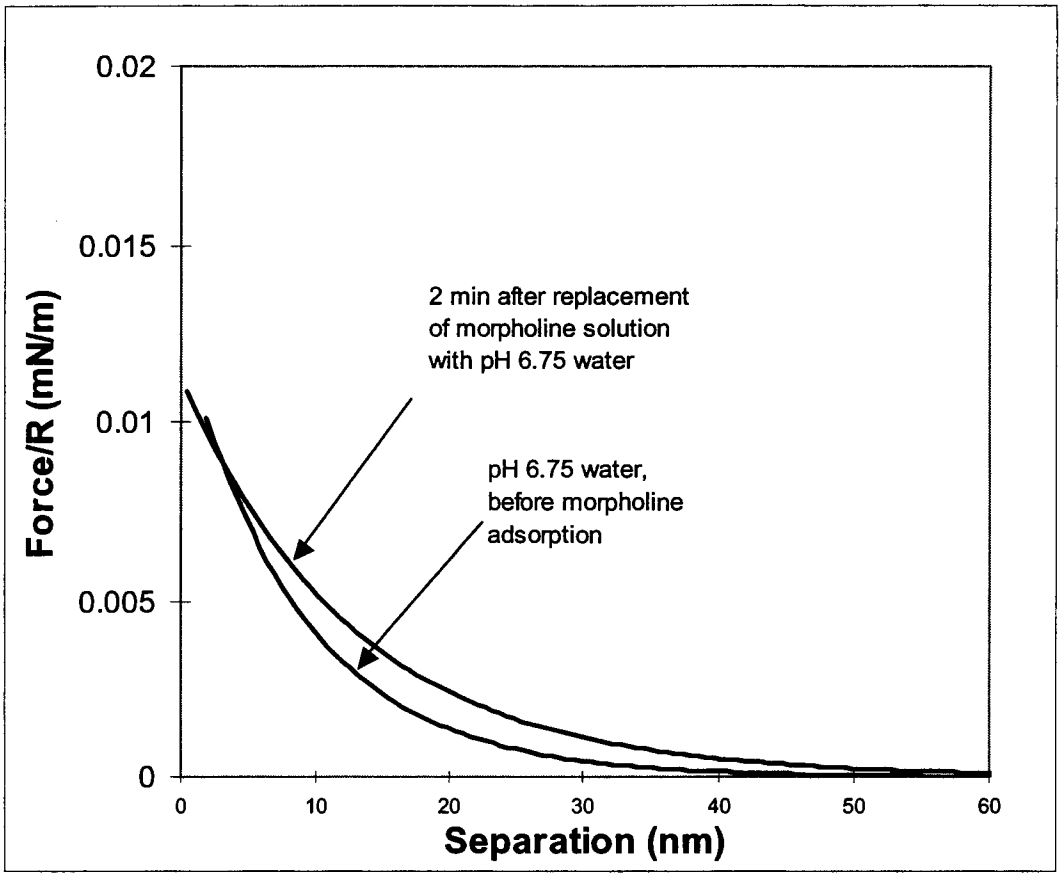

Figure 2-11: Comparison of force curves measured before exposure to a 50 mg/kg solution of morpholine and within 2 min of flushing the cell with morpholine-free water at the same pH.

2.2.2 DMA Adsorption/Desorption near the PZC of Magnetite

The net force between the surfaces of Alloy 600 and magnetite changed slowly with time with the introduction of a 50 mg/kg (1.1 mM) solution of DMA at pH_{25} 6.75. To the extent that the force curve is affected by the adsorption of DMA, this result suggests that the adsorption of DMA onto the surface of magnetite is relatively slow, which is consistent with the adsorption behaviour measured by Laser Raman Spectroscopy (see section 2.1.1). The raw force data are shown in Figure 2-12. After 10 min, the net force between the surfaces of Alloy 600 and magnetite is essentially zero for all separations down to ≈ 4 nm, at which point some parts of the surfaces come into contact and the force becomes strongly repulsive. Within 25 min of exposure to the DMA solution, however, the net force between the surfaces of Alloy 600 and magnetite has become attractive. The force curve continued to change over the course of the next 30 min, although the net force remained attractive throughout this period of time.

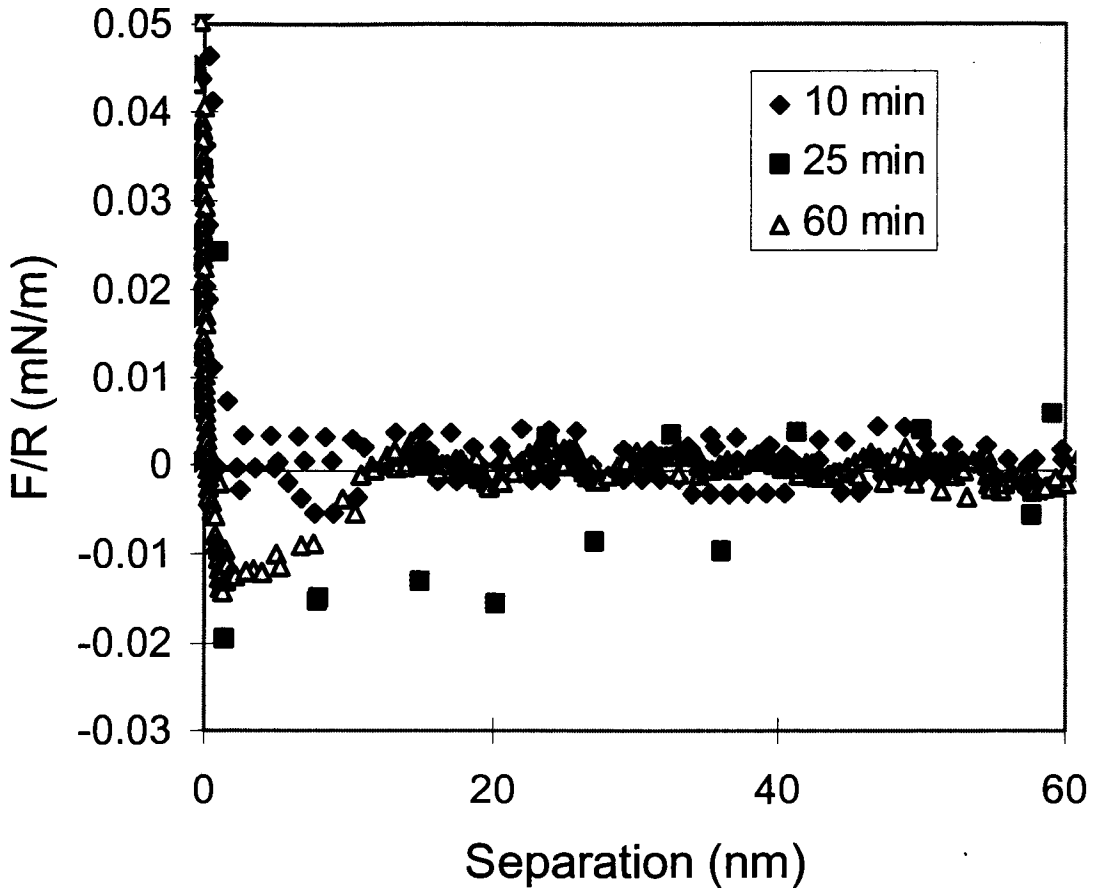

Figure 2-12: Force between the surface of Alloy 600 and a magnetite particle as a function of separation at selected exposure times to a 50 mg/kg solution of DMA at pH_{25} 6.75.

The desorption data acquired after the replacement of the 50 mg/kg solution of DMA with DMA-free water at the same pH are shown in Figure 2-13. In contrast to the behaviour with morpholine (where within 2 min the force curve was essentially the same as that measured before the introduction of the morpholine solution), the force curve underwent a complex set of changes similar to those observed during the 60 min exposure to DMA. After 60 min the force curves were still changing, and a further addition of DMA-free water at pH_{25} 6.75 produced still further changes.

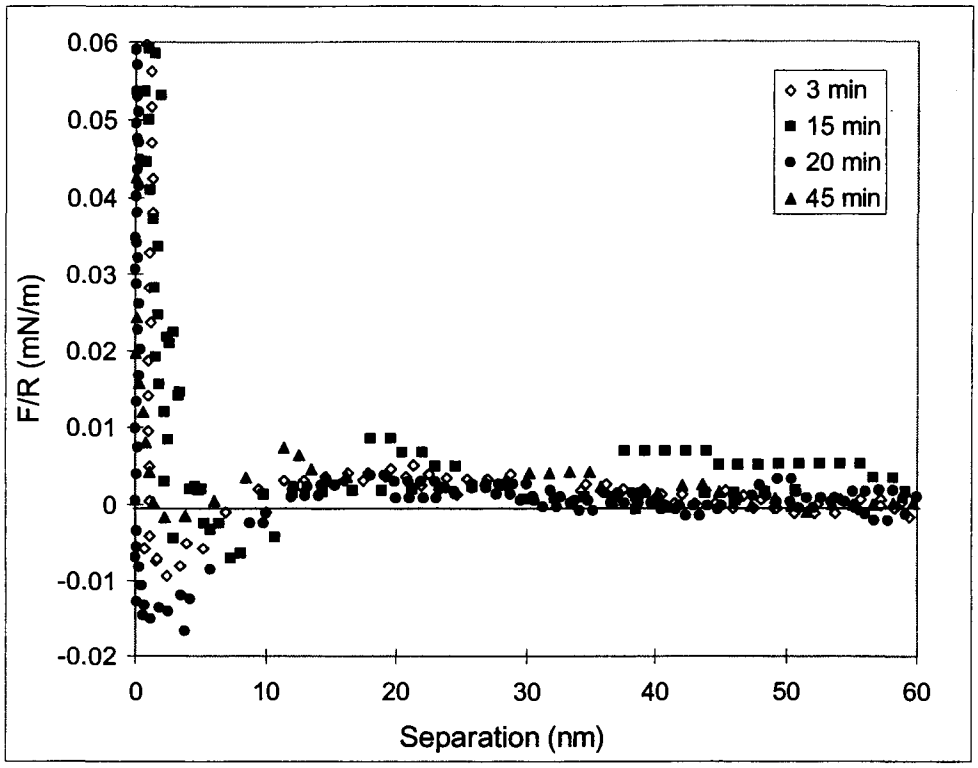

Figure 2-13: Force between the surface of Alloy 600 and a magnetite particle at pH_{25} 6.75 as a function of separation at selected times after flushing DMA from the cell.

2.2.3 Dimethylamine Adsorption/Desorption at pH_{25} 10

The force curves at selected times following the introduction of a 50 mg/kg solution of DMA at pH_{25} = 10 are shown in Figure 2-14. In the absence of DMA the force between the surfaces of magnetite and Alloy 600 is strongly negative at pH_{25} 10, as expected from previous work. The immediate effect, i.e., within the first 10 min, of introducing a 50 mg/kg solution of DMA, however, is to reduce the repulsive force to such an extent that the net force between the surfaces becomes attractive at distances greater than about 5 nm. Within 1 h the net force is again repulsive, but with a smaller magnitude than before DMA was added. The force curves measured after 1 h are similar to those reported previously for this system (Turner et al., 1999).

The response of the net force curve to replacing the 50 mg/kg solution of DMA with distilled water at pH_{25} = 10 is shown in Figure 2-15. The initial response is for the repulsive force to decrease from the value it reached after 1 h exposure to the DMA solution. Within 20 min, however, the repulsive force has increased towards its initial value before introducing the DMA solution. At this time a second addition was made of distilled water at pH_{25} 10, which caused the repulsive force to decrease again.

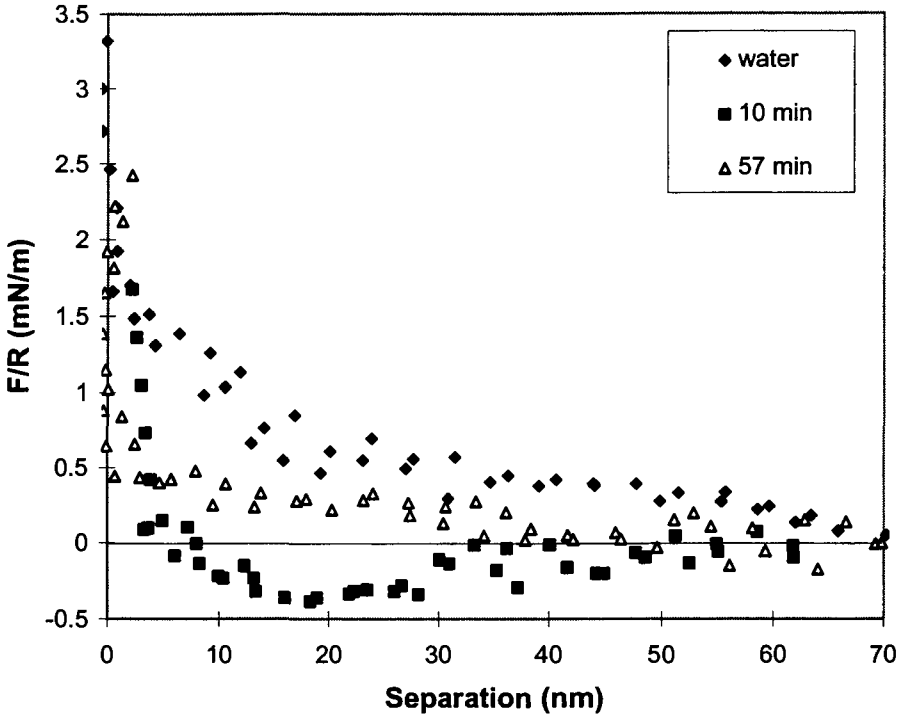

Figure 2-14: Force between the surface of Alloy 600 and a magnetite particle as a function of separation for selected exposure times to a 50 mg/kg solution of DMA at pH_{25} 10.

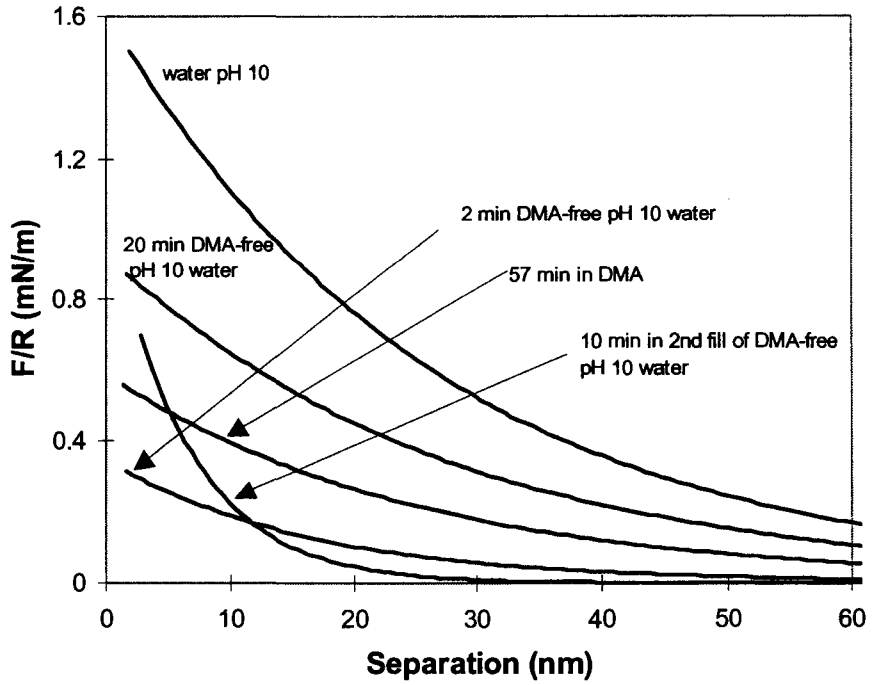

Figure 2-15: Force between the surface of Alloy 600 and a magnetite particle at pH_{25} 10 as a function of separation at selected times after flushing DMA from the cell.

2.3 Surface Contact Angle

The results of measurements of the contact angle (θ) of 50 mg/kg solutions of morpholine and DMA at surfaces of Alloy 600 and magnetite for selected temperatures between 25°C and 190°C are shown in Figure 2-16. The cosine of the contact angle is plotted because this quantity is proportional to the change in the free energy of the interface. The dashed and dotted lines are for measurements made on the projected image of the meniscus for solutions of DMA and morpholine, respectively. The solid line is cosine of the average of the contact angles at surfaces of Alloy 600 and magnetite for a solution of DMA, where the contact angles were measured from photographs (See Figures 2-18 and 2-19, below). Several trends are illustrated in Figure 2-16. First, the contact angles measured between the steam-water interface and the surface of Alloy 600 are higher (cosθ less positive) than the contact angles at the surface of magnetite. Second, the contact angles for solutions of morpholine are generally higher (cosθ less positive) than those for solutions of DMA. Finally, all of the interfaces (i.e., solutions of DMA or morpholine contacting substrates of Alloy 600 or magnetite) become more hydrophobic (cosθ becomes less positive) as temperature increases, and tend towards being non-wetting at about 160°C.

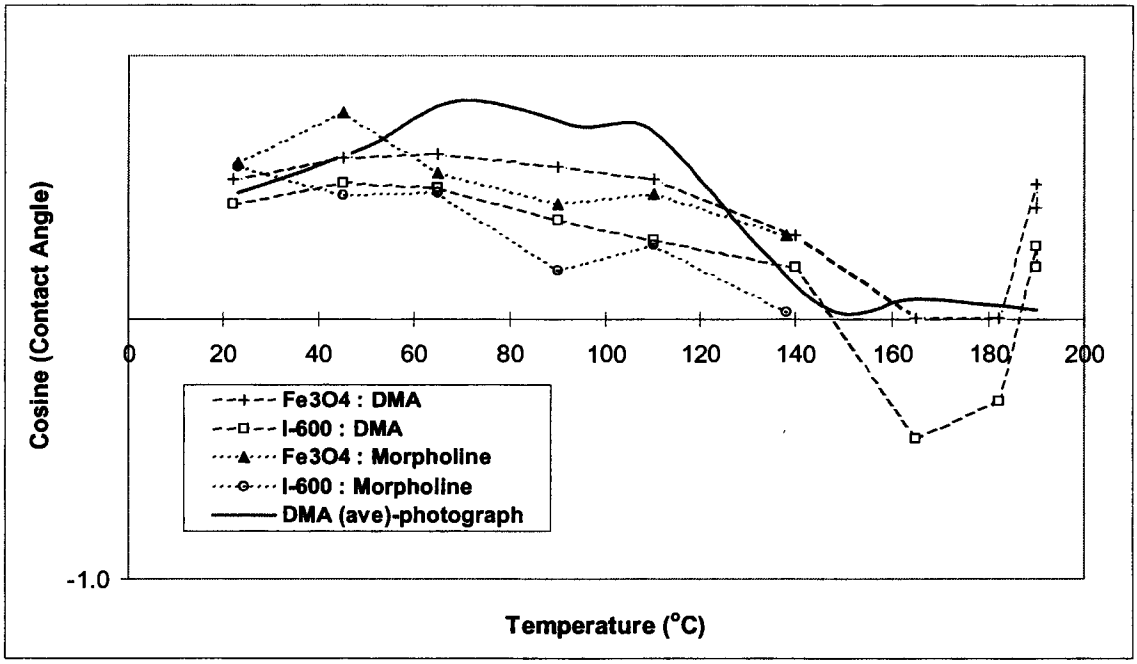

Figure 2-16: Cosine of contact angles measured as a function of temperature for solutions of DMA and morpholine contacting surfaces of Alloy 600 and magnetite.

The cosine of the contact angles measured from projected images of the meniscus of the pure water-steam interface on surfaces of Alloy 600 and magnetite are shown in Figure 2-17 for comparison. As with the solutions of amine, the contact angles are higher (cosine of the contact angle less positive) at the surface of Alloy 600 than at magnetite, suggesting that the difference is associated with a property of water and not of the amine. Figure 2-17 also shows that pure water does not tend to become more hydrophobic with increasing temperature, as do the solutions of amine (compare Figure 2-16).

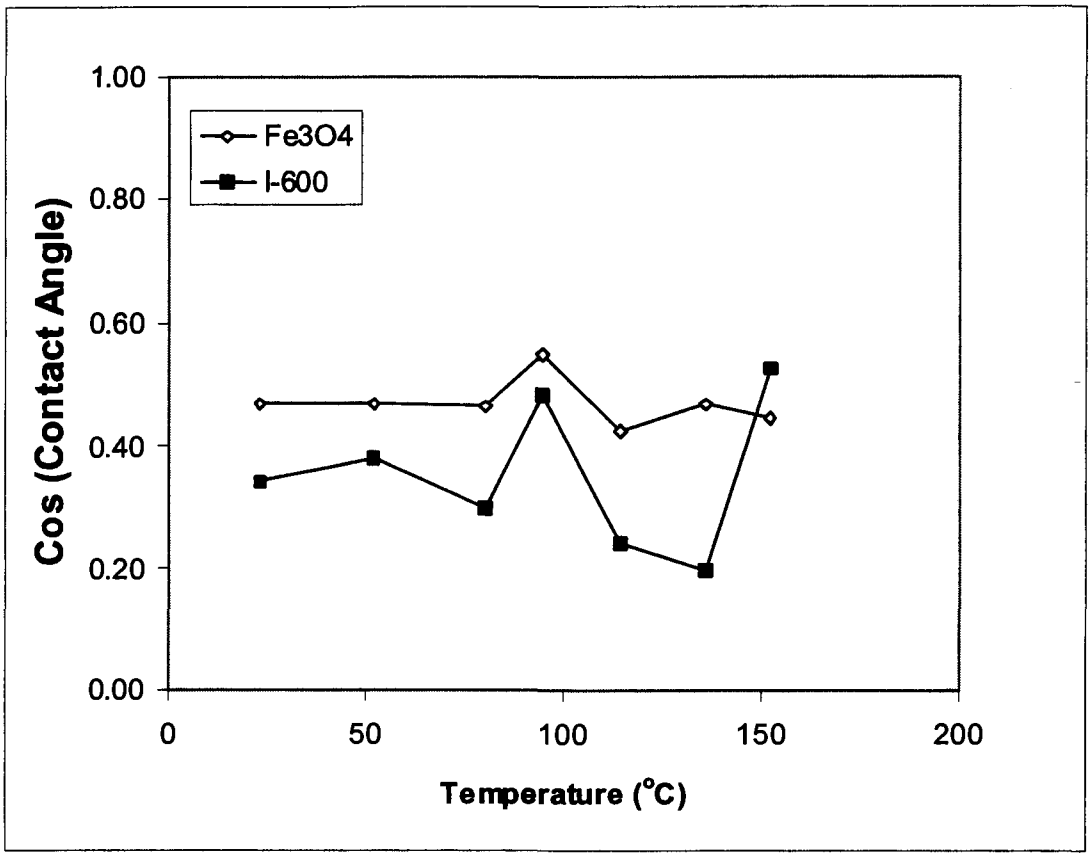

Figure 2-17: Cosine of contact angles measured as a function of temperature for pure water at the surfaces of Alloy 600 and magnetite.

Photographs of the meniscus formed between a 50 mg/kg solution of DMA and the surfaces of Alloy 600 and magnetite at selected temperatures are shown in Figures 2-18 and 2-19. In the photographs, the meniscus appears as an opaque curved band extended between the vertical surfaces of Alloy 600 (on the left) and a single crystal of magnetite (on the right). The phase above the meniscus is vapour (DMA + steam) and the phase below the meniscus is liquid (DMA + water).

The decrease in the contact angle (the angle measured in the liquid phase between the solid surface and the meniscus) when the temperature is raised from 25°C to 70°C is clearly illustrated in Figure 2-18. A further increase in solution temperature from 70°C to 95°C results in a modest increase in the magnitude of the contact angle. The increase in contact angle when the solution is heated from 100°C to 145°C is more striking, as illustrated in Figure 2-19. The meniscus forms a right angle with the surfaces of both Alloy 600 and magnetite at temperatures of 145°C, 165°C and 190°C, indicating that the solution is non-wetting on these surfaces over the stated temperature range.

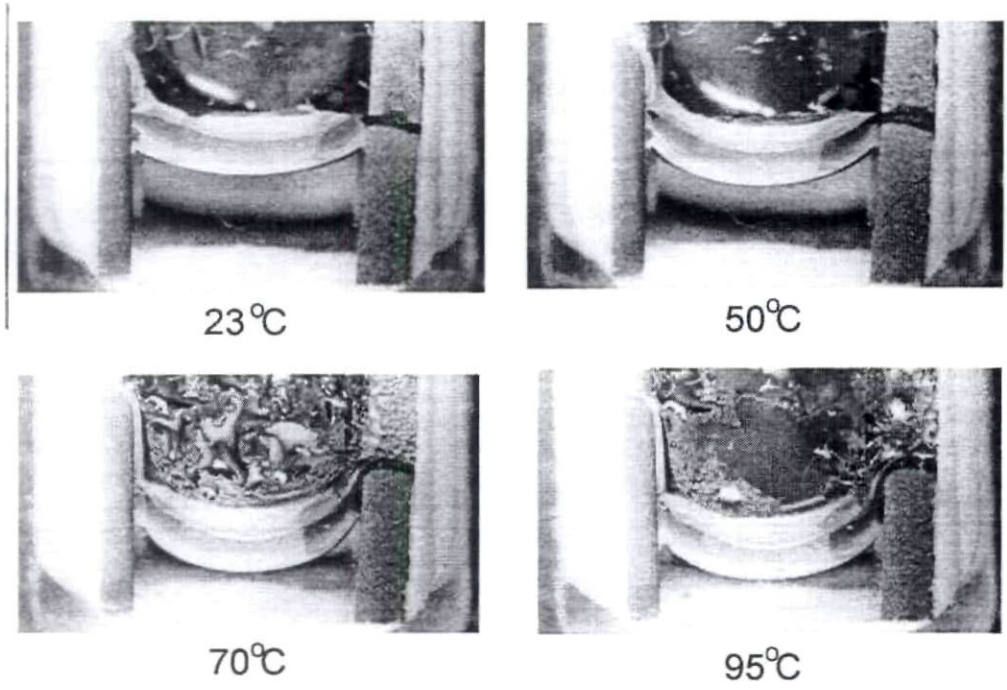

Figure 2-18: Photographs taken at 23°C, 50°C, 70°C, and 95°C of the meniscus formed between solutions of DMA and surfaces of Alloy 600 and magnetite. Alloy 600 is on the left in the photograph and magnetite is on the right.

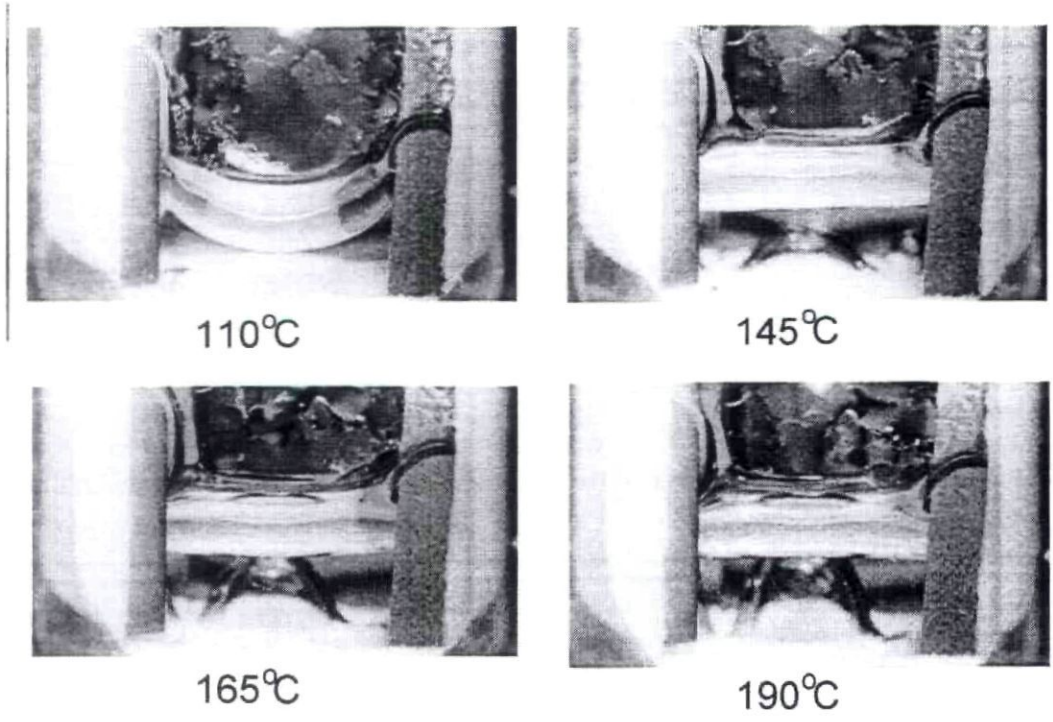

Figure 2-19: Photographs taken at 110°C, 145°C, 165°C, and 190°C of the meniscus formed between solutions of DMA and surfaces of Alloy 600 and magnetite. Alloy 600 is on the left in the photograph and magnetite is on the right.

2.4 Loop Fouling Tests

The results of the loop tests to determine the effect of the amine concentration on the rate of particuate fouling are summarized in Table 2-1 and in Figures B-1 to B-8 in Appendix B. In previous investigations (Turner et al., 1997; Turner et al., 1999), the initial rate of deposit build-up was reported as a deposition rate because it was thought that the build-up rate only depended upon factors that influence the rate constant for particle deposition. New insights suggest that the initial rate of deposit build-up can also be influenced by rate constants for particle removal and deposit consolidation (Turner and Klimas, 2001), hence the initial rate of deposit build-up will be referred to in this report as a fouling rate, rather than a deposition rate. Normalized fouling rates (fouling rate per unit particle concentration) are reported in Table 2-1 for both flow-boiling regions of the test section and regions where the flow regime is forced convection.

The region of the test section of most interest is the flow-boiling section where steam quality ranges from 0 to 0.25 because this is most representative of the tube bundle in the steam generator. A comparison of the data from the region of interest shows that the fouling rates measured in tests with morpholine chemistry are higher than those measured with DMA. In addition, the trend in fouling rate with amine concentration is opposite for DMA to that observed with morpholine.

Apart from test D137, where the normalized fouling rate appears to be anomalously high for X = 0.05 - 0.15 (see Figure B-2), the average fouling rates over the range $0 < X < 0.25$ for tests with morpholine chemistry control are as follows:

- Morpholine = 50 mM, average fouling rate = 4.8×10^{-4} kg/m^2·s.
- Morpholine = 5 mM, average fouling rate = 3.4×10^{-4} kg/m^2·s.

The results appear to be independent of the acid used to prepare the buffered solutions (see Table 1-3 for chemistry conditions established for each test). In comparison, the average normalized fouling rates over the range $0 < X < 0.25$ for tests under DMA chemistry control are:

- DMA = 50 mM, average fouling rate = 3.08x10-5 kg/m2·s.
- DMA = 5 mM, fouling rate = 7.80x10-5 kg/m2·s.

Table 2-1: Summary of results from loop fouling tests.

Exp.	Amine Conc.	Normalized Fouling Rate Flow Boiling (kg/m^2·s)		Normalized Fouling Rate Forced Convection (kg/m^2·s)			
		0 < X < 0.25	X ≈ 0.5	Single Phase	X ≈ 0.05	X ≈ 0.25	X ≈ 0.55
Morpholine Chemistry							
D136	Low	2.30×10^{-4}	5.57×10^{-3}	3.34×10^{-4}	2.08×10^{-4}	2.87×10^{-4}	1.37×10^{-4}
D137	High	1.40×10^{-3}	4.23×10^{-5}	3.16×10^{-4}	1.80×10^{-4}	1.96×10^{-4}	3.90×10^{-4}
D144	Low	4.55×10^{-4}	1.01×10^{-1}	5.64×10^{-4}	3.67×10^{-4}	2.04×10^{-4}	1.15×10^{-3}
D145	High	5.93×10^{-4}	3.93×10^{-2}	2.48×10^{-4}	7.86×10^{-4}	5.79×10^{-4}	3.60×10^{-4}
D146	High	3.63×10^{-4}	-	2.75×10^{-4}	2.06×10^{-4}	1.13×10^{-4}	-
Dimethylamine Chemistry							
D138	Low	7.80×10^{-5} *	6.46×10^{-4}	1.21×10^{-4}	2.10×10^{-4}	3.22×10^{-5}	3.14×10^{-4}
D139	High	2.73×10^{-5}	6.68×10^{-5}	2.10×10^{-4}	2.94×10^{-4}	2.70×10^{-5}	3.30×10^{-5}
D147	High	3.42×10^{-5}	2.43×10^{-3}	1.74×10^{-4}	2.77×10^{-4}	3.85×10^{-5}	1.11×10^{-4}

*: Average for 0.055<X<0.25

The activity of 59-Fe measured by the on-line gamma detector TS2 (X ≈ 0.20) as a function of time during tests D136 and D146 for fouling under morpholine chemistry control is shown in Figures 2-20 and 2-21, respectively. The data illustrated are representative of what was measured by gamma detectors TS1 and TS3 on these and the other tests conducted with morpholine chemistry control (D137, D144-146). For times prior to t = 0 h the water is circulating in the loop at the test operating conditions, but since the magnetite injection has not yet started the on-line gamma detector is measuring residual background activity from deposit on the loop tubing from previous tests. Injection of magnetite begins at t = 0 h and thereafter the activity on the test section increases at a constant rate, signifying a constant rate of particle fouling onto the test section. The deposit activity on the test section remains relatively constant after the injection pump is switched off (at t= 32 h and t = 50 h for tests D136 and D146, respectively), signifying that the rate of particle removal is relatively low for tests conducted under morpholine chemistry control. The relative rates of deposition and removal were not affected by the concentration of morpholine in either the carboy or the loop or by the acid used to prepare the morpholine buffer solution. At the end of the removal phase, the loop is switched off and the test section removed for off-line measurements of deposit distribution along the test section. Measurements of residual activity for t = 51 - 53 h shows loop background at levels close to those prior to the test.

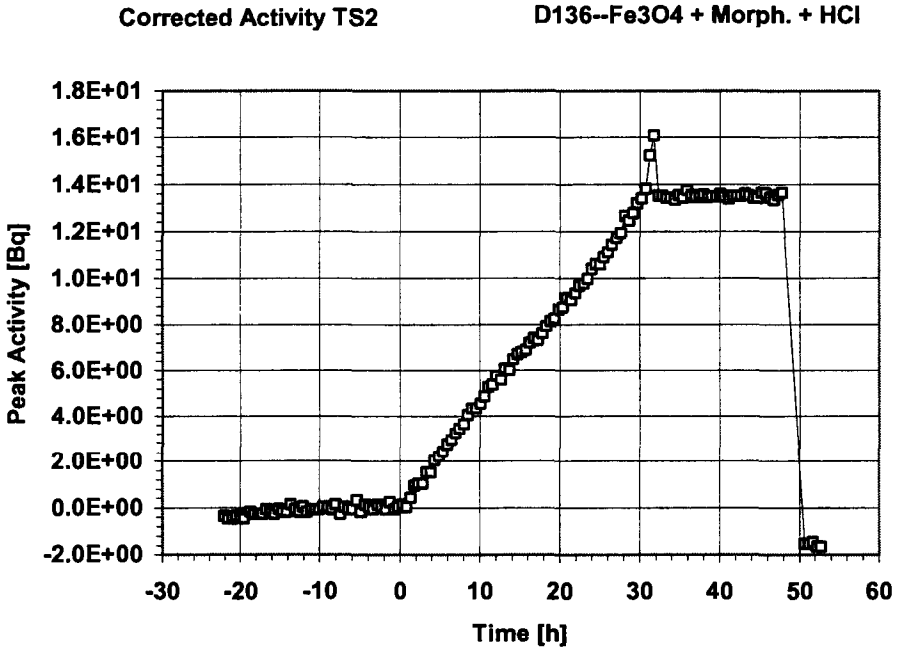

Figure 2-20: Time dependence of the deposit activity measured on the test section by gamma detector TS2 (steam quality ≈ 0.20) for experiment D136.

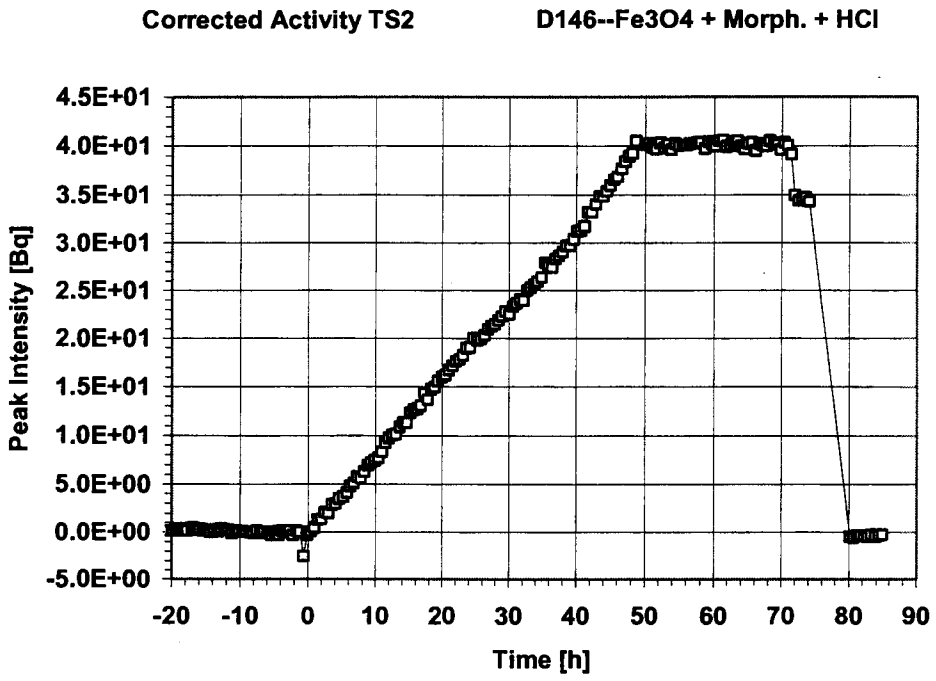

Figure 2-21: Time dependence of the deposit activity measured on the test section by gamma detector TS2 (steam quality ≈ 0.20) for experiment D146.

The activity of 59-Fe measured by the on-line gamma detectors as a function of time during tests D138 and D147 for fouling under DMA chemistry control is shown in Figures 2-22 and 2-23, respectively. Both figures show that the loop background activity decreased slowly for times prior to t = 0 h, suggesting that the DMA chemistry was gradually mobilizing loop deposit from previous tests and transporting it out of the loop before the start of magnetite injection. Following the start of magnetite injection at t = 0 h the deposit activity increased at a constant rate, signifying a constant rate of fouling onto the test section. Once the injection of magnetite into the loop was stopped, however, (at t ≈ 48 h for both tests D138 and D147) the deposit activity decreased with time at a rate that is much higher than was observed for the tests conducted using morpholine chemistry. For test D138 the measurement of deposit removal was interrupted after only 3 h by a loop trip. For D147, however, the measurements of deposit activity during the removal phase of the test continued for a period of 40 h, and showed clearly that the rate of deposit removal with DMA chemistry is significantly higher than the rate measured under morpholine chemistry control. Measurements of residual activity after the test section was removed from the loop (t = 100 - 106 h for test D147) showed that the loop background was much lower than at the start of the test. In fact, a linear extrapolation of the loop activity measured from t = -20 h to t = 0 h intersects the loop activity measured at t = 100 h, suggesting that deposit removal from the loop tubing continued throughout the test period.

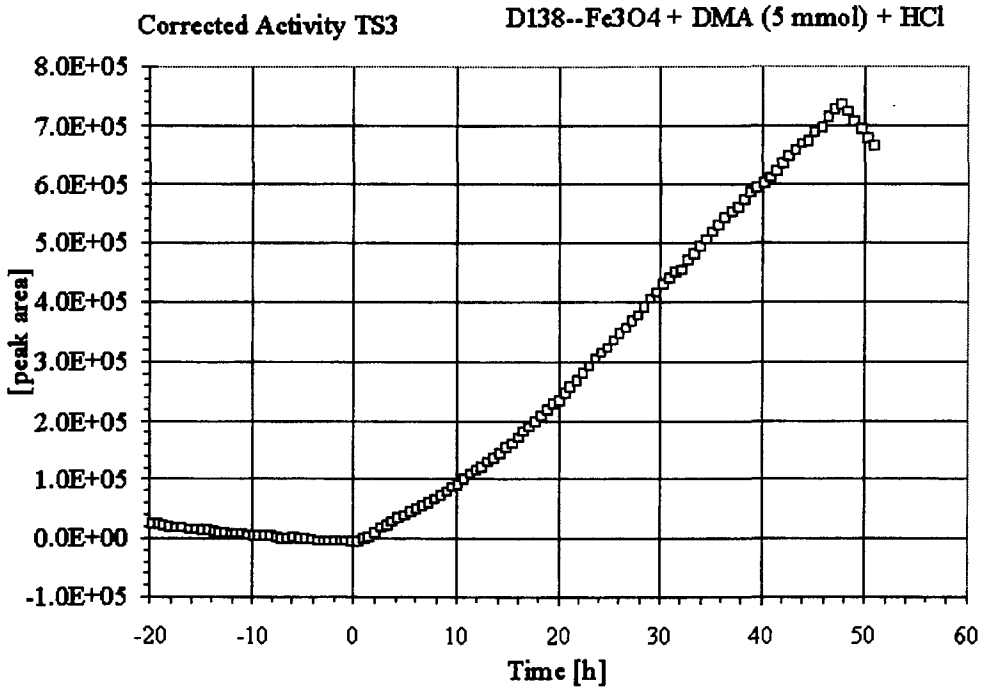

Figure 2-22: Time dependence of the deposit activity measured on the test section by gamma detector TS3 (steam quality ≈ 0.40) for experiment D138.

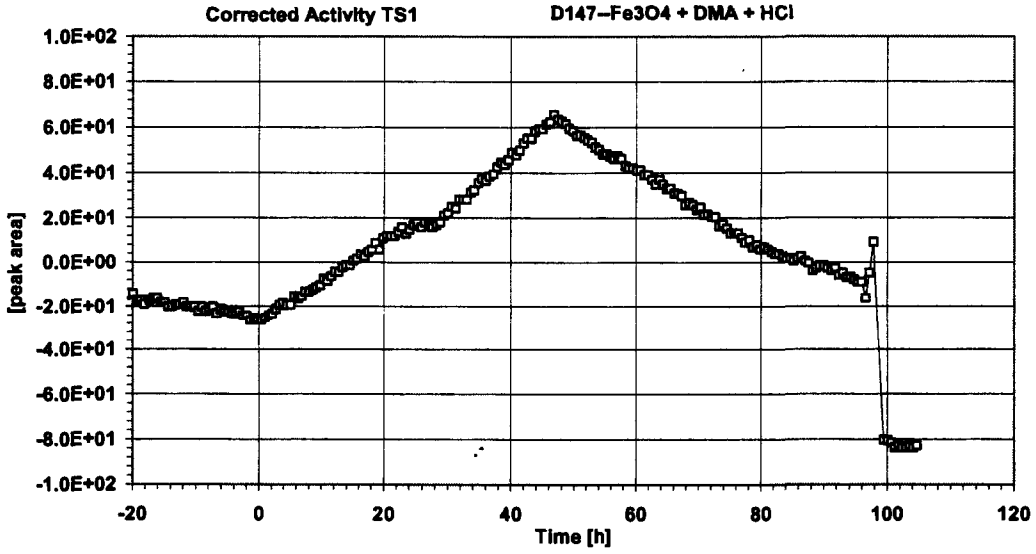

Figure 2-23: Time dependence of the deposit activity measured on the test section by gamma detector TS1 (steam quality ≈ -0.20) for experiment D147.

3. DISCUSSION

3.1 Adsorption and Desorption Kinetics

The results of the measurements of surface concentration by Laser Raman Spectroscopy (LRS) show that both morpholine and DMA adsorb slowly onto the surface of magnetite at pH 10 and 25°C. Morpholine adsorbed at the rate of 0.20 mmole·g^{-1}·min^{-1} before reaching a plateau after approximately 30 min. The total amount adsorbed is in good agreement with previous results where the samples were equilibrated with a solution of amine for a period of 24 h before measurements were made (Turner et al., 1999). The rate of DMA adsorption was 0.12 mmole·g^{-1}·min^{-1} for the first 10 min, and then fell to about one third of that rate. A plateau was not reached within the 60-min exposure time, which may account for why the total amount adsorbed was less than half of that expected from previous results.

Desorption of both morpholine and DMA from the surface of magnetite is significant at temperatures greater than 100°C, although the desorption kinetics of the two amines are very different. Desorption of morpholine is so rapid that the surface concentration had essentially reached steady state by the time the first measurement was made (5 min heating time + 5 min to attain thermal equilibrium) with only small changes in concentration thereafter. The surface concentration of morpholine at t = 0 (i.e., the time of the first measurement after thermal equilibrium had been established) decreases exponentially with temperature with a temperature coefficient of 0.0176. Thus:

$$C_s(T) = C_s^{\circ} \exp(-0.0176\ T). \quad (4)$$

DMA desorbed much more slowly from the surface of magnetite such that it typically required 10 to 20 min to reduce the surface concentration by a factor of 2. At no temperature did the surface concentration of DMA reach steady-state within the 20-min measurement period. The surface concentration of DMA at t = 0 (reflecting the small quantity of amine that did desorb during the 10 min required for heat-up and thermal equilibration) decreases exponentially with temperature with a temperature coefficient of 0.00184. Thus:

$$C_s(T) = C_s^{\circ} \exp(-0.00184\ T). \quad (5)$$

Atomic Force Microscopy (AFM) measurements show that changes to the net force between the surfaces of magnetite and Alloy 600 following either the addition or removal of amine from solution occur over similar time scales to those observed for the adsorption/desorption of amine as measured by LRS. This result strongly suggests that the changes in the net force are associated with the adsorption/desorption of amine. Similarity of the results from LRS (adsorption/desorption) and AFM (interaction force) also shows that the desorption behaviour is independent of whether desorption is initiated by an increase in temperature (as with the LRS measurements) or by a reduction in the concentration of amine in solution (as with the AFM measurements). The desorption kinetics also appear to be independent of pH.

The force between magnetite and Alloy 600 at pH 6.75 and 25°C is weakly repulsive, as expected for a metal oxide at a pH slightly greater than its PZC. Recall, for the purpose of this discussion, that the total force between two surfaces immersed in a liquid is equal to the sum of

the van der Waals dipole force and a force associated with surface charge (Hiemenz, 1977). The van der Waals force is normally attractive, whereas the force associated with the surface charges can be either repulsive (for surfaces of like charge) or attractive (for surfaces of opposite charge). Since an adsorbed layer of molecules will have only a negligible effect on the van der Waals force, changes in the net force curve accompanying the adsorption or desorption of amine at 25°C are interpreted as a reflection of the effect the adsorbed amine is having on the surface change. Amine exists in solution as both the neutral molecule, A, and as its conjugate acid, HA^+. Adsorption of the latter onto the negatively charged surface of magnetite (or Alloy 600) will tend to reduce the magnitude of the repulsive force between magnetite and Alloy 600, and hence make the net force between these two surfaces less repulsive.

The effect of the adsorption of morpholine onto the surface of magnetite at pH_{25} 6.75 in the tests reported here is difficult to interpret because the net force between magnetite and Alloy 600 became more repulsive following addition of the morpholine solution. This is inconsistent with previous results where, as expected, adsorption of morpholine made the net force less repulsive over the entire pH range examined (Turner et al, 1999). Adsorption of DMA at pH_{25} 6.75 reduced the repulsive component of the force between magnetite and Alloy 600, as expected from previous results. Close examination of the force curves in Figure 2-12, however, shows that the repulsive component of the net force drops initially then recovers somewhat as adsorption of DMA proceeds. A similar sequence is observed during desorption (see Figure 2-13), where the repulsive force first drops between 15 and 20 min then rises again to a higher value after 45 min. The changes in the net force during adsorption/desorption of DMA at pH_{25} 10 are similarly complex. The net force between magnetite and Alloy 600 at pH 10 and 25°C is strongly repulsive, as expected for a metal oxide at a pH significantly greater than its PZC. During the adsorption of DMA, however, the net force first becomes attractive (suggesting effective neutralization of the negative charge on magnetite) within 10 min exposure to the solution of DMA before switching back to being repulsive again at 57 min. Although the overall effect of adsorption of DMA is to make the net force less repulsive, the repulsive component of the force drops significantly during the early stages of adsorption and then recovers somewhat as adsorption proceeds. Figure 2-15 shows the same pattern of change during desorption at pH_{25} 10.

The complex sequence of changes to the net force between magnetite and Alloy 600 that occur as a function of time during the adsorption and desorption of DMA are perhaps associated with rearrangement of the adsorbate molecules either on the surface or within the adsorbed layers. It is interesting to note that with DMA the adsorption and desorption kinetics were both slow and were accompanied by a complex sequence of changes to the net force curve. The response of the force curve to the adsorption of morpholine, although equally slow to that of DMA, is hard to interpret and inconsistent with previous results, as noted above. The relatively fast response to the removal of morpholine, however, suggests that desorption of this molecule does not proceed via the complex processes that apparently take place with DMA.

3.2 Effect of Amine on Particle Fouling

The fouling tests were designed to test the hypothesis that the dependence of the magnetite fouling rate on the amine used for pH control is related to the effect that the adsorbed amine has on the particle surface charge (Turner et al., 1997). Adsorption of amine at room temperature

reduces the force of repulsion between magnetite and Alloy 600 by reducing the surface charge on magnetite, so it follows that greater adsorption of amine should lead to higher fouling rates. This explanation appeared to account for the difference in fouling rates between tests conducted under DMA and morpholine chemistry control, and was consistent with the previous observation that fouling rates were consistently higher in tests performed with elevated concentrations of amine (necessitated by the presence of an acidic impurity in the cover gas used during equilibration of the magnetite suspension with amine).

The fouling tests reported here, however, do not confirm the previous observation that the fouling rate of magnetite particles is higher at elevated concentrations of amine. The acids selected to prepare the constant pH_T buffer solutions for this investigation (see Table 1-3) were chosen because they contained non-complexing and relatively non-adsorbing anions. In this way, any surface-charge effects should be associated solely with adsorption of the amine. In previous tests, however, where the effect of amine concentration was first noted, the acidic impurity in the cover gas was likely carbon dioxide. Carbon dioxide is known to adsorb onto the surface of metal oxides, and this adsorption may be responsible for the different behaviour observed previously.

Figure 3-1 shows a plot of normalized particle fouling rate as a function of the concentration of morpholine and DMA. The figure includes all data reported in this investigation (Turner et al., 1997; Turner et al., 1999) except from tests that had a suspected CO_2 contamination in the cover gas. Although there is a small tendency for the fouling rate to increase with increasing concentration of morpholine, the effect is not very strong. For DMA, however, the fouling rate decreases significantly with increasing concentration of DMA. The absence of a strong trend with morpholine could simply mean that at 270°C morpholine is such a weak base that its adsorption does not influence the surface charge of magnetite. A similar conclusion can be drawn from the work of Wesolowski et al. (1999) based on the absence of an effect of morpholine concentration on the PZC of magnetite at high temperature. The trend in fouling rate with concentration of DMA, however, is opposite to that expected from surface-charge effects. This result suggests that some other mechanism (not related to surface charge) is responsible for the effect of the concentration of DMA on the magnetite particle fouling rate and, by implication, for the difference between the effectiveness of DMA and morpholine as deposit-control reagents at constant pH_T.

Additional insights into the mechanism by which the choice of amine affects the fouling rate of magnetite particles come from observations of the rate at which deposit is removed from the test section during the removal phase of each test (See Equations 1 – 3 and Figures 2-20 to 2-23). The data in Figures 2-20 to 2-23 show distinct differences in the removal behaviour of magnetite particles depending on the amine used for pH control. For example, essentially no deposit is removed from the test section during the removal phase of the tests when morpholine is used to control the pH (see Figures 2-20 and 2-21). In comparison, a significant amount of deposit is removed from the test section in tests where pH is controlled using DMA (see Figures 2-22 and 2-23). The kinetics of particle removal were investigated independently by AECL at the Chalk River Laboratories over the past several years. A fouling model has been developed on the basis of these studies in which deposit removal is the result of two independent processes; hydrodynamic removal and consolidation (Klimas and Turner, 2001). Consolidation is described

as the process whereby deposit increases in density and becomes more strongly bound to the surface. In the model, it is assumed that only the fraction of deposit that has not yet become consolidated is available to be removed by the fluid flow. Thus, a low rate of deposit removal correlates with a high rate of deposit consolidation, and vice versa. The removal behaviour illustrated in Figures 2-20 to 2-23 suggests that the rate of consolidation of the magnetite deposit is significantly higher in tests with morpholine pH control than in those tests where pH is controlled using DMA. The implications of this difference in the rate of consolidation on the rate of tube-bundle fouling are examined using predictions by the AECL fouling model in Section 4.

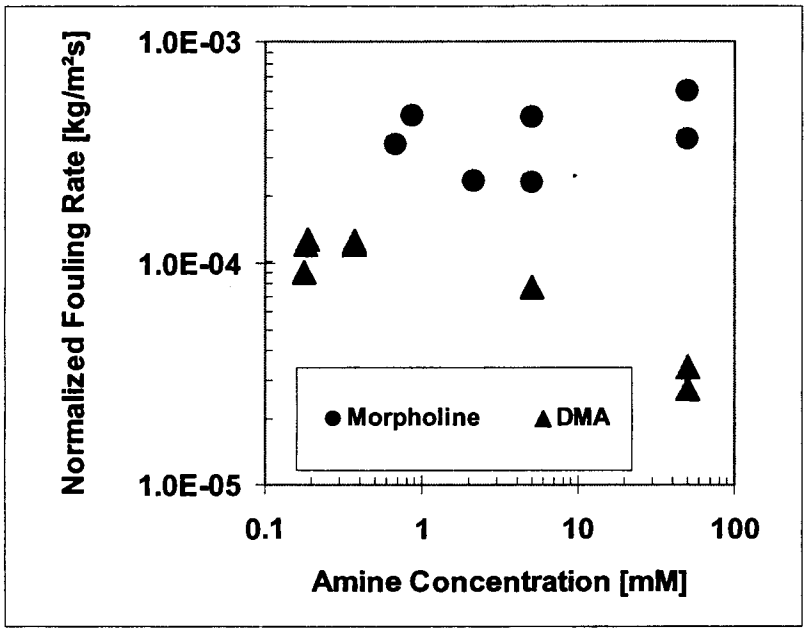

Figure 3-1: Normalized fouling rate of magnetite particles under flow-boiling conditions versus concentration of amine.

3.3 Contact Angle and Hydrophobicity

Contact angle is the angle measured in solution between a solid surface and a liquid/vapour interface. It is a measure of how well a liquid 'wets' a solid surface. For contact angle <90° ($1 > \cos\theta > 0$), the liquid is said to wet the surface and the surface is labelled hydrophilic. Contact angle > 90° ($0 > \cos\theta > -1$) means the liquid is 'non-wetting' and the surface is described as being hydrophobic. It has been noted previously (Balakrishnan et al, 1998) that polymeric dispersants both reduce the particle fouling rate and reduced the wall superheat for bubble nucleation under flow-boiling conditions. The latter effect suggests that the dispersant has adsorbed onto the heat transfer surface and made it more hydrophobic (Collier, 1972). One can infer from this result that, in general, additives that make the heat transfer surface more hydrophobic may be expected to lower the rate of particle fouling in addition to reducing the wall superheat under flow-boiling conditions.

Both amines tended to make the surfaces of magnetite and Alloy 600 more hydrophilic than pure water at temperatures less than 120°C, whereas the surfaces were more hydrophobic at temperatures greater than 120°C. The difference in contact angle between the solutions of morpholine and DMA was small, however, over the temperature range measured. In addition, the wall superheat measured in the loop fouling tests did not show a dependence on the amine used for pH control (Turner et al., 1997). Therefore, differences in the hydrophobic character of the surface that may be associated with the amine used for pH control do not appear to be sufficient to account for the reduction in the fouling rate of magnetite particles with DMA compared to the rate with morpholine.

4. SUMMARY AND IMPLICATIONS FOR FOULING CONTROL

Previous work on this project has demonstrated that the rate of particle fouling under flow-boiling conditions is strongly influenced by surface chemistry (Turner et al., 1997; Turner et al., 1999). The effect of surface chemistry is illustrated by the difference between the fouling rates of magnetite and hematite, and by the influence of the amine used for pH control on the fouling rate of magnetite. The relative fouling rates of magnetite and hematite are consistent with their respective surface charges, with positively-charged hematite fouling at a rate that is more than 10 times greater than for that measured for negatively-charged magnetite at the same pH_T. Having noted that the effectiveness of the amine at reducing magnetite fouling is roughly in proportion to base strength, it was hypothesized that the amine affects the fouling rate by adsorbing onto the particles and reducing their surface charge. Subsequent measurements at 25°C confirmed that adsorption of amine made magnetite particles less negative. Thus, the hypothesis appeared to be plausible. A third way in which surface chemistry may affect the particle fouling rate was revealed by an investigation of the mitigating effect of dispersants on particle fouling (see Section 3.3). Test results suggested that reagents that make the surface more hydrophobic may be expected to reduce the rate of particle fouling as well.

Additional loop tests reported here have confirmed that DMA results in a lower magnetite particle fouling rate than does morpholine. Tests done as a function of amine concentration at constant pH_T, however, do not support the hypothesis that the amine affects the particle fouling rate via its influence on the surface charge. The same holds true for the effect of amine on the hydrophobic nature of the heat transfer surface. Measurements showed that the amines do make the surface more hydrophobic at elevated temperature, which should tend to reduce the rate of particle fouling. However, the difference between the hydrophobicity of surfaces exposed to solutions of DMA and morpholine does not appear to be sufficient to account for the difference between the particle fouling rates.

The scope of the investigation was expanded this time to include measurements of the kinetics of adsorption/desorption of amine from the surface of magnetite, and of the kinetics of particle removal from the heat transfer surface. The measurements revealed distinctive differences in behaviour between tests performed with DMA and morpholine. Both DMA and morpholine adsorb slowly onto the surface of magnetite at room temperature and tend to desorb once the temperature is increased beyond 100°C. The desorption kinetics of DMA, however, are at least 10 times slower than they are for morpholine. In addition, the rate of particle removal from the heat transfer surface was significantly greater in tests with DMA than with morpholine. These differences have strong implications for how different amines might affect fouling behaviour in an operating plant.

Figure 4-1 shows the effect of temperature on the desorption of morpholine and DMA from the surface of magnetite as predicted by Equations (4) and (5), respectively. As discussed in Section 3.1, the equations capture the short-term effects, i.e., the desorption that occurs within several min of heating to the temperature of interest, for a suspension of particles that has first been equilibrated with amine at 25°C. The curves shown in Figure 4-1 for both DMA and morpholine are independent of time to a first approximation; for DMA because the desorption kinetics are slow compared to the residence time of a particle being transported with the feedwater, and for

morpholine because the desorption kinetics are so fast that the amount of morpholine adsorbed on a particle quickly equilibrates at the local temperature of interest.

During their residence time in the condenser hot-well (approximately 30 min, depending on the design of the steam-cycle) amine will adsorb onto the surface of the magnetite particles. The particles are then transported with the feedwater through a series of low-pressure and high-pressure feedwater heaters where they are heated with the fluid to the final feedwater temperature. Total transit time in the feedtrain is only a few min (depending on the design of the steam cycle), so Equations (4) and (5) should apply. Figure 4-1 shows that for final feedwater temperatures ranging from 180°C to 220°C, approximately 80% of the morpholine that adsorbed in the condenser hot-well will have desorbed before the particles reach the steam generator. In contrast, the particles will have lost only 20% of the DMA molecules that adsorbed in the condenser hot-well because of the significantly lower desorption kinetics of DMA. These results suggest that the desorption kinetics of the amine may be an important factor in determining the effectiveness of amines as deposit-control reagents in the steam generator.

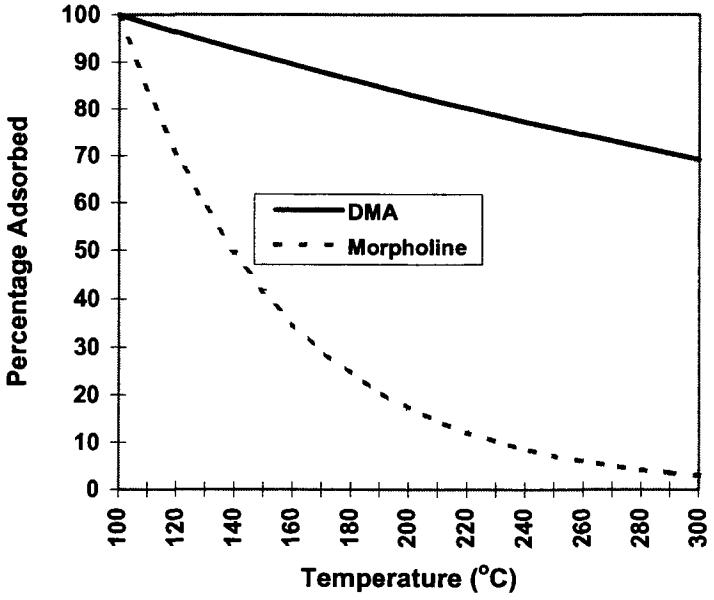

Figure 4-1: Percentage of amine adsorbed as a function of temperature following equilibration with amine at 25°C.

Another factor that distinguishes the behaviour of DMA from that of morpholine is the effect on the rate of particle removal. As noted in Section 3.2, pH control with DMA results in a significantly higher rate of particle removal than is observed when pH is controlled with morpholine. This effect has been investigated independently by AECL, and the lower rate of removal is attributed to a higher rate of deposit consolidation when morpholine is used to control pH. The effect of the rate of deposit consolidation on the over-all particle fouling rate is illustrated in Figure 4-2. Details of the analysis are published elsewhere (Turner and Klimas, 2001).

All three curves were generated using the same rate constants for particle deposition and removal. The only difference amongst the three curves is the relative magnitudes of the rate constants for hydrodynamic removal and consolidation. The highest rate of deposit build-up is observed when the rate constant for consolidation is 10 times greater than the rate constant for hydrodynamic removal. In this case, most of the particles become consolidated before they have a chance to be removed and the rate of deposit build-up becomes essentially equal to the rate of particle deposition. The intermediate fouling rate corresponds to the case where the rate constants for removal and consolidation are identical. The lowest fouling rate is observed for the case where the rate constant for consolidation is significantly less than the rate constant for hydrodynamic removal. In this case, most of the deposit remains un-consolidated and, therefore, is subject to hydrodynamic removal. It is interesting to note that the fouling rate is linear in all three cases. This is not a general result, and is dependent upon the rate constants for removal and consolidation. In traditional analyses of the fouling process (which do not take consolidation into account), a linear fouling rate is interpreted as signifying that the rate of removal is small compared to the rate of deposition (Epstein, 1988). The added insight from this analysis is that differences in linear fouling rate, which would otherwise have been attributed to the rate of particle deposition, may in fact be a result of differences in the rate of deposit consolidation on the heat transfer surface.

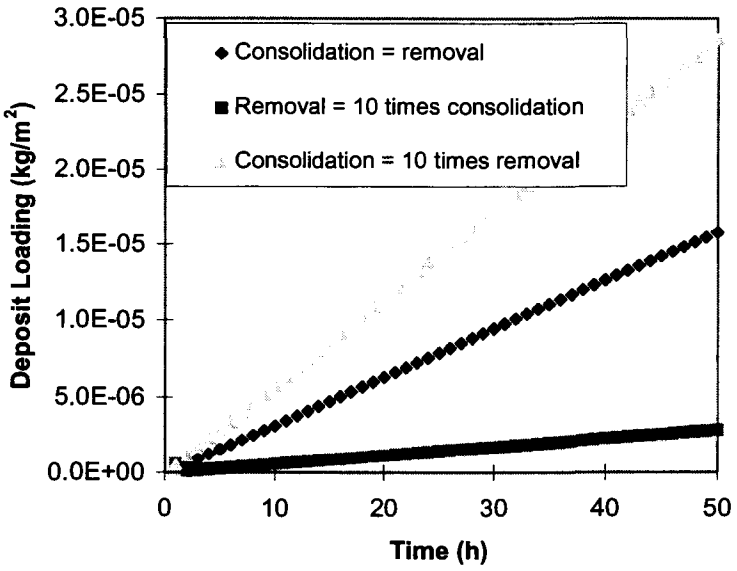

Figure 4-2: The effect of the relative rate constants for hydrodynamic removal and consolidation on the particle fouling rate.

The desired properties or characteristics that an amine must have to achieve good deposit and chemistry control are listed in Table 4-1, along with the rational for why that particular property is important. Properties #1 and #2 combined will ensure that materials throughout the steam-cycle and especially those in the two-phase regions of the steam cycle will be protected against corrosion. Properties #3 and #4 correlate with an amine that produces a low fouling rate under flow-boiling conditions. Property #5 may be an important factor in why dispersants are effective

at reducing fouling under flow-boiling conditions. DMA embodies all of the properties except #2; it is too volatile to be used on its own for pH-control in the steam-cycle. One option is to combine DMA with another less volatile amine to achieve good deposit and chemistry control. A second option is to modify DMA with other functional groups to reduce its volatility and increase its hydrophobicity, without otherwise sacrificing its effectiveness, and thereby achieve superior deposit and chemistry control with one chemical reagent.

Table 4-1: Desired properties of an amine for good deposit and chemistry control throughout the steam-cycle.

#	Property	Rational
1	Strong base at high temperature	Maintain alkaline chemistry at high temperature
2	Low volatility	Protect steam generator crevices and materials exposed to condensate
3	Strongly adsorbed; slow desorption kinetics	Remain adsorbed on particles during transport to steam generator
4	High rate of particle removal; slow rate of consolidation	Reduces fouling rate
5	Hydrophobic	Reduces fouling rate

5. CONCLUSIONS AND SUGGESTIONS FOR FUTURE INVESTIGATION

5.1 Conclusions

Conclusions from the experimental program to determine the effect of alternative amines on the rate of tube-bundle fouling are:

- Particle fouling rates are a strong function of water and surface chemistry. For example:
    - Fouling rates by hematite are approximately 10 times higher than that of magnetite.
    - Both hematite and magnetite fouling rates are sensitive to the level of oxygen/hydrazine in water. In the presence of residual oxygen/no hydrazine, the magnetite fouling rates increase. Under no oxygen and with residual hydrazine, the hematite fouling rates decrease towards those of magnetite.
    - Magnetite fouling rates are the lowest (for steam quality < 35%) when water pH is controlled with DMA. Furthermore, the fouling rates decrease with increasing DMA concentration, supporting the hypothesis of a causal link between the presence of DMA and the reduced fouling rates.
    - Low fouling rates in the presence of DMA are accompanied by high removal rates of deposited particles.
    - The high fouling rates that were observed during the initial investigation were apparently caused by the presence of an unidentified acidic impurity, likely carbon dioxide. The hypothesis that these high fouling rates were caused by high concentrations of amines (needed for pH control in the presence of the acidic impurity) has not been verified.
- Particle fouling rates are a strong function of thermohydraulic conditions. For example:
    - The fouling rate under single-phase forced convective is low.
    - The fouling rate under subcooled nucleate boiling is high under some chemistries.
    - The fouling rate under saturated nucleate boiling conditions is moderate.
    - The fouling rate under flow-boiling conditions at high steam quality (commencing at steam qualities of greater than 35%) is very high. A mechanism to account for the high fouling rate in this flow regime has been proposed (Turner et al., 1999).

- Overall fouling rates are postulated to be the resultant of three independent processes:
  - deposition
  - re-entrainment
  - consolidation

A decrease in fouling rate could be caused by any one of the following: a decrease in deposition rate, an increase in the re-entrainment rate, a decrease in the rate of consolidation. Chemistry can affect the overall fouling rate by influencing any one of these processes. It appears most likely that the differences between the fouling rate of magnetite and hematite are related to the effect of surface charge on the deposition process. Differences in magnetite fouling rate from one amine to another appear to be related to the effect of the amine on the consolidation process. These differences are manifested in the ease with which deposited particles are subsequently removed from the surface by hydrodynamic forces.

- Adsorption of amines affects surface chemistry and fouling behaviour of corrosion products. Thus:
  - Adsorption of amine makes the surface less negative. This is manifested as a reduction in the force of repulsion between magnetite and I 600 under alkaline conditions where both magnetite and I 600 are negatively charged.
  - Amines desorb from the surface of corrosion products with increasing temperature, but the rate of desorption varies with the amine.
  - There may be a correlation between a low rate of desorption from the corrosion product and a low rate of deposit consolidation.

Key conclusions from the investigations to date (Turner et al., 1997; Turner et al., 1999; the present report) of the effect of amines on tube-bundle fouling are listed in Table 5-1, below.

Table 5-1: Key conclusions from investigations of surface chemistry and the effect of amines on the rate of tube-bundle fouling.

Key Conclusions
• Fouling rate is strongly dependent upon surface charge. This accounts for why hematite particles deposit at a significantly higher rate than magnetite particles. • Fouling rate depends upon the amine used for pH control for steam quality < 35%. Fouling rate with DMA is 3 times lower than with morpholine. • Additives that make the surface more hydrophobic may be expected to reduce the rate of particle fouling and reduce wall superheat. • Deposit removal rate is significantly higher with DMA than with morpholine.

Key Conclusions
• There appears to be a correlation between slow amine desorption kinetics, a high particle removal rate, and a low particle fouling rate. The link between these three processes could be the influence of the amine on the rate of particle consolidation (Turner and Klimas, 2001), i.e., the amine cannot inhibit consolidation if it has desorbed from the surface. The distinguishing feature of amines that promotes a low desorption rate may be the absence of hydrophilic groups on the amine, e.g., DMA versus morpholine or ethanolamine.

5.2 Suggestions for Future Investigation

- Future loop fouling tests should extend the measurements of deposit removal rate to enable a full analysis to be made of all three components of fouling: deposition, re-entrainment and consolidation. Details of the analysis are described in Turner and Klimas (2001), and will shed light on the effect of chemistry and thermohydraulic conditions on these three processes.
- Measure the fouling rates in the presence of amines structurally similar to DMA, for example trimethylamine, diethylamine, triethylamine, dipropylamine.
- Incorporating work already performed which identified a list of amines recommended for a field trial based on optimized properties for BOP chemistry (EPRI TR-100755, 1992), develop a short-list of amines to identify structural features important for slow desorption kinetics at high temperature.
- Investigate the possibility of chemical reaction (surface dissolution?) between iron corrosion products and DMA.
- Measure the deposition, re-entrainment and consolidation rates as a function of concentration of DMA in the presence of other amines (e.g, ETA or morpholine) to develop a practical mixed-amine water chemistry optimized for fouling mitigation.
- Conduct measurements of fouling at high steam quality using a different mass flux, so as to verify the previously proposed mechanism of fouling at steam qualities greater than 35%.

6. NOMENCLATURE

C	concentration (moles/m^2)
T	temperature (K)
m	deposit mass (kg/m^2)
t	time (s)
λ	removal coefficient (s^{-1})
θ	contact angle

Subscripts

c	consolidation
r	removal

7. REFERENCES

Balakrishnan, P.V., S.J. Klimas, L. Lépine, and C.W. Turner (1998). "Polymeric Dispersants For Control of Steam Generator Fouling". 3rd International Steam Generator and Heat Exchanger Conference, June 21-24, 1998, Toronto, Canada. AECL-11975, COG-99-165-I.

Beal, S.K. and Chen, J.H. (1986). "A Model of Sludge Behaviour in Nuclear Plant Steam Generators". Electric Power Research Report EPRI NP-4620.

Bénézeth, P., D.J. Wesolowski, and D.A. Palmer (2000). "Effects of Dimethylamine on the Surface charge Properties of Magnetite", Electric Power Research Institute Report 1001029, EPRI, Palo Alto, CA (2000).

Cobble, J.W. and Turner, P.J. (1992), "PWR Advanced All-Volatile Treatment Additives, By-Products, and Boric Acid", Electric Power Research Institute Report EPRI TR 100755, EPRI Palo Alto, CA.

Collier, J.G. (1972). Convective Boiling and Condensation, McGraw-Hill Book Company New York.

Epstein, N. (1988), "General Thermal Fouling Models". Fouling Science and Technology, eds. L.F. Melo, T.R. Bott, and C.A. Bernardo, NATO Advanced Science Institute Series, Kluwer Academic Press, London.

Hiemenz, P.C. (1977). Principles of Colloid and Interface Science Marcel Dekker, Inc. New York.

Schoonen, M.A.A. (1994). "Calculation of the Point of Zero Charge of Metal Oxides between 0 and 350°C", Geochimica et Cosmochimica Acta **58** pp. 2845-2851.

Turner, C.W. and S.J. Klimas, and M.G. Brideau (1997). "The Effect of Alternative Amines on the Rate of Boiler Tube Fouling". Electric Power Research Institute Report EPRI TR 108004, EPRI, Palo Alto, CA, (1997).

Turner, C.W., D.A. Guzonas, and S.J. Klimas (1999). "Surface Chemistry Interventions to Control Boiler Tube Fouling". Electric Power Research Institute Report TR-110083, EPRI, Palo Alto, CA, (1999).

Turner, C.W. and S.J. Klimas (2001). "Modelling the Effect of Surface Chemistry on Particulate Fouling under Flow-Boiling Conditions", Heat Exchanger Fouling: Fundamental Approaches and Technical Solutions, 2001 July 8-13, Davos, Switzerland.

Wesolowski, D.J., D.A. Palmer, P. Benezeth, and C. Xia (1999). "Effects of Morpholine on the Surface Charge Properties of Magnetite", Electric Power Research Institute Report TR-110082, Palo Alto, CA, (1999).

Appendix A

CALCULATION OF ADSORBED AMINE FROM NORMALIZED RAMAN SPECTRA

All spectra measured at 25°C were normalized to the intensity of the perchlorate band at 938 cm^{-1}. For each spectrum measured at a temperature greater than 25°C, a temperature-dependent scaling factor, F_T, was calculated from the intensity of the perchlorate band at 938 cm^{-1} using:

$$I_{25}^{p} = F_T I_T^{p}$$

where I_{25}^{p} is the intensity of the perchlorate band at 25°C and I_T^{p} is the intensity of the perchlorate band at temperature T. F_T was then used to scale the intensities of the bands corresponding to CH stretching modes on the amine molecule in the same sample. Thus:

$$I_s^{CH} = F_T I_T^{CH}$$

The quantity of amine removed from solution by adsorption onto magnetite is then calculated from the difference, $I_{s,diff}^{CH}$, between the scaled intensities of the CH stretching mode in the absence and presence of magnetite, i.e.

$$I_{s,diff}^{CH} = I_{s,reference}^{CH} - I_{s,magnetite}^{CH}$$

The quantity of amine adsorbed in grams per gram of magnetite is given by

$$c_{absorbed} = \frac{I_{S,diff}^{CH} \cdot V \cdot MW}{Jm}$$

where V is the volume of solution in the Raman cell, MW is the molecular weight of the amine, m is the mass of the magnetite in contact with the solution, and J is a calibration constant relating the Raman intensity to amine concentration (Turner et al., 1999).

Appendix B

RESULTS OF LOOP FOULING TESTS

Test conditions that are not listed in Table 1-3 in the text for each loop test are listed in Table B-1 below.

Table B-1
Conditions used for the loop tests

Exp.	pH		Magnetite (mg/kg)		Thermalhydraulics		
	Loop	Carboy	Loop	Carboy	Pressure (MPa)	Heat Flux (kW/m^2)	Mass Flux ($kg/m^2 \cdot s$)
D-136	9.69	9.58	0.44	157	5.7	226	281
D-137	9.72	9.65	0.34	156	5.6	220	304
D-138	10.32	10.29	0.34	196	5.5	246	292
D-139	10.45	10.36	0.34	140	5.6	175	287
D-144	9.68	9.45	0.16	126	5.8	226	314
D-145	9.59	9.69	0.24	99	5.9	221	312
D-146	9.58	9.68	0.26	70	5.8	213	311
D-147	10.14	10.33	0.24	63	5.9	220	311

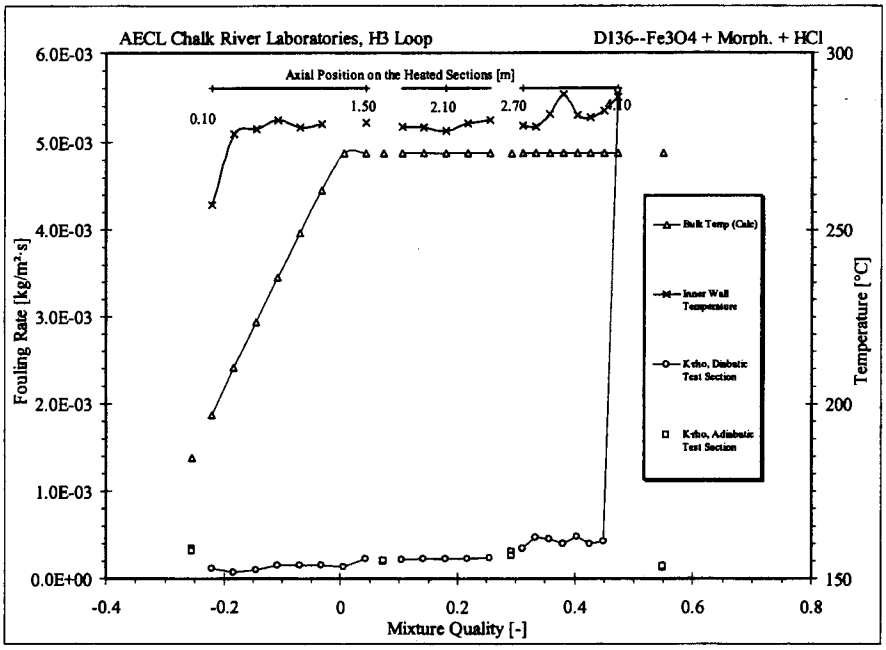

Figure B-1 **Normalized fouling rate versus steam quality. ○ indicates locations along the heated (diabatic) section, □ indicates locations on the unheated (adiabatic) sections.**

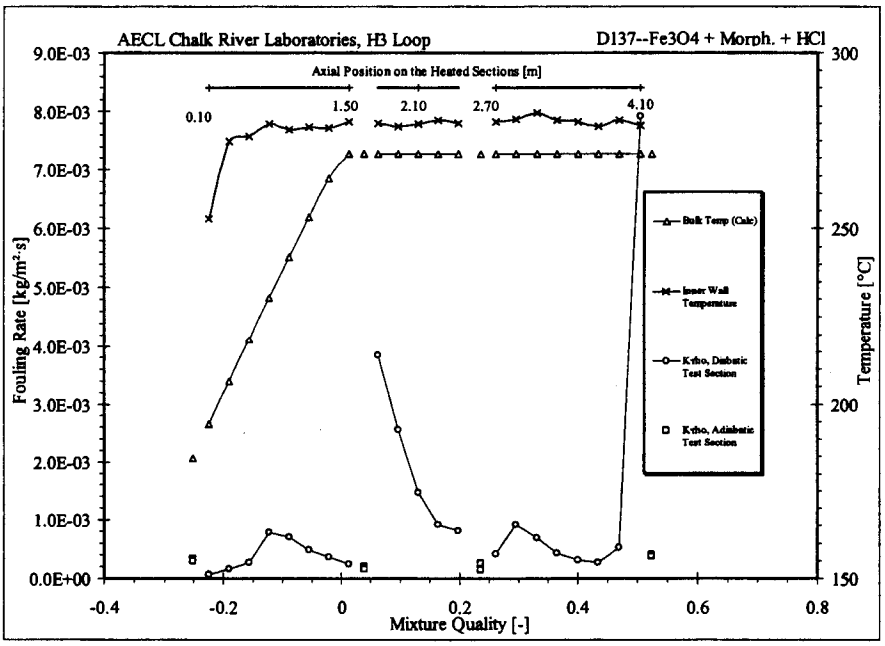

Figure B-2 **Normalized fouling rate versus steam quality. ○ indicates locations along the heated (diabatic) section, □ indicates locations on the unheated (adiabatic) sections.**

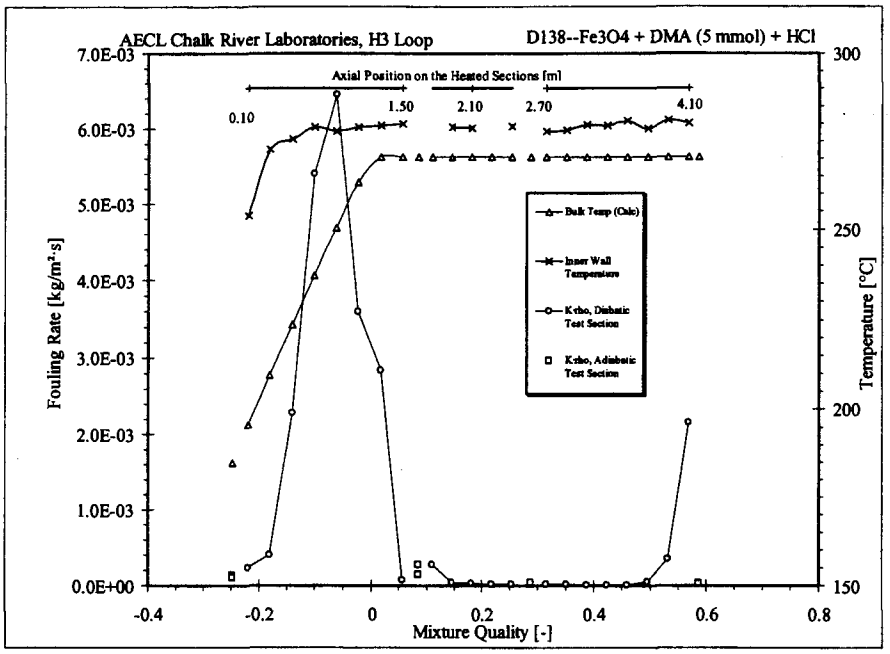

Figure B-3 **Normalized fouling rate versus steam quality. ○ indicates locations along the heated (diabatic) section, □ indicates locations on the unheated (adiabatic) sections.**

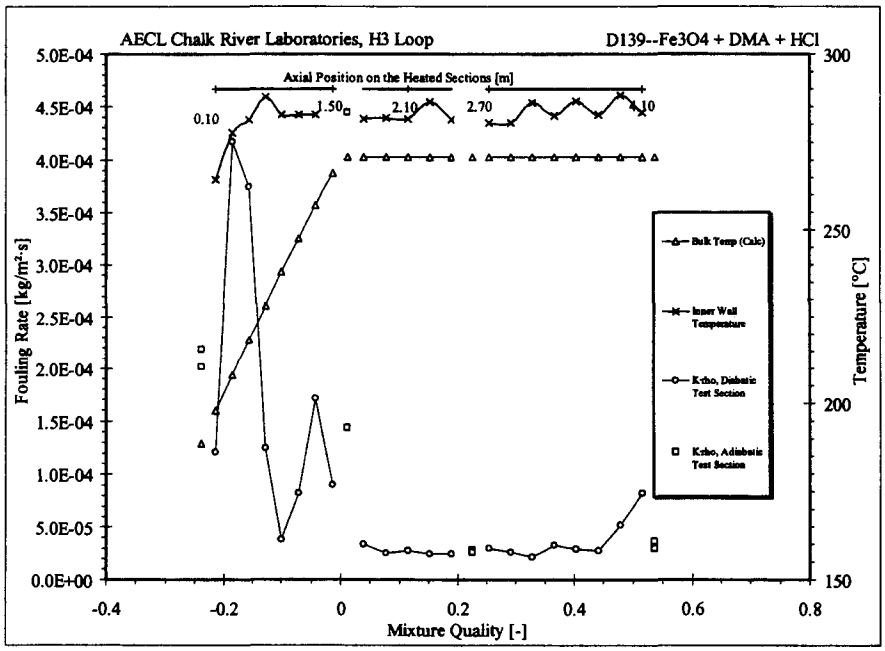

Figure B-4 **Normalized fouling rate versus steam quality. ○ indicates locations along the heated (diabatic) section, □ indicates locations on the unheated (adiabatic) sections.**

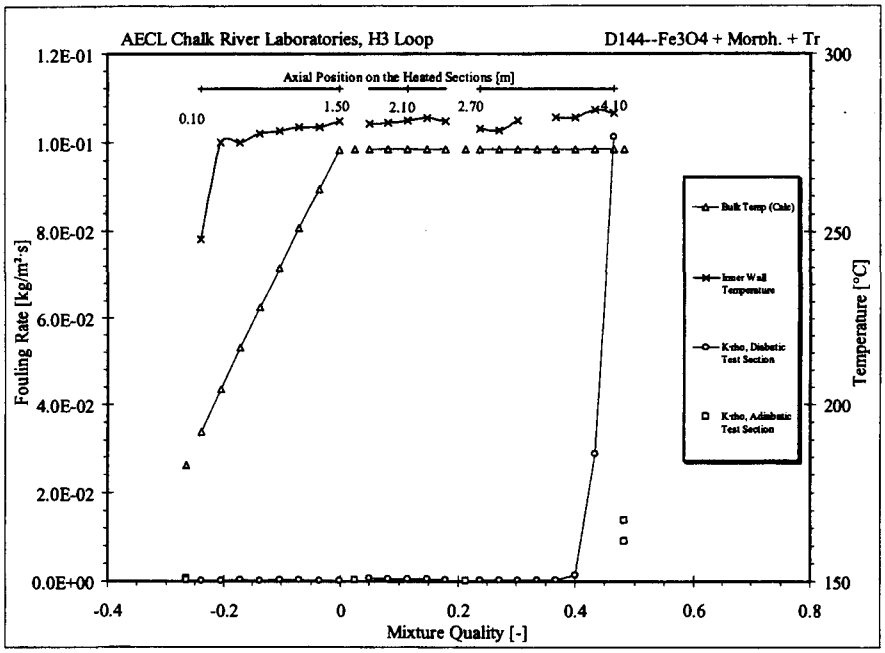

Figure B-5 **Normalized fouling rate versus steam quality. ○ indicates locations along the heated (diabatic) section, □ indicates locations on the unheated (adiabatic) sections.**

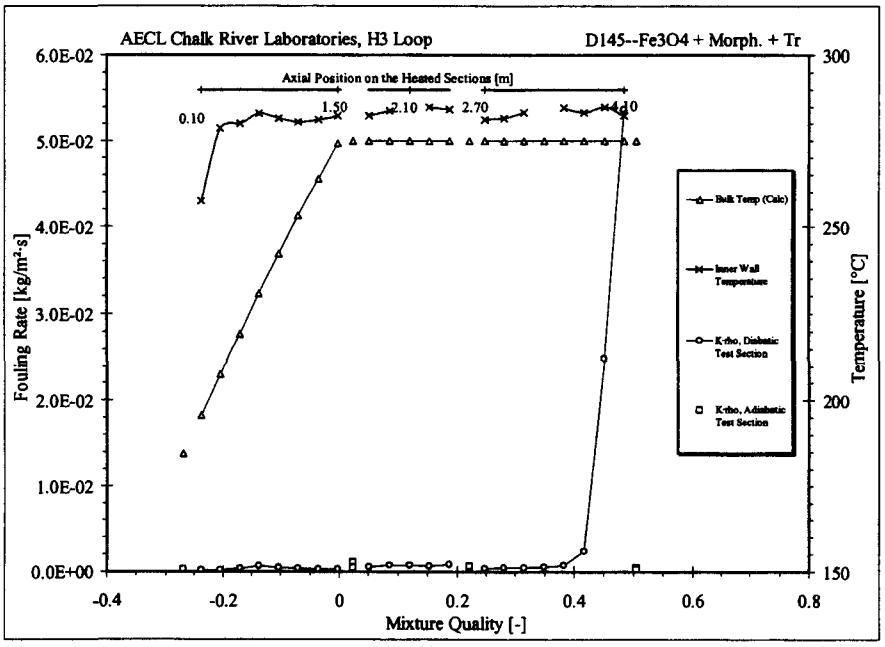

Figure B-6 **Normalized fouling rate versus steam quality. ○ indicates locations along the heated (diabatic) section, □ indicates locations on the unheated (adiabatic) sections.**

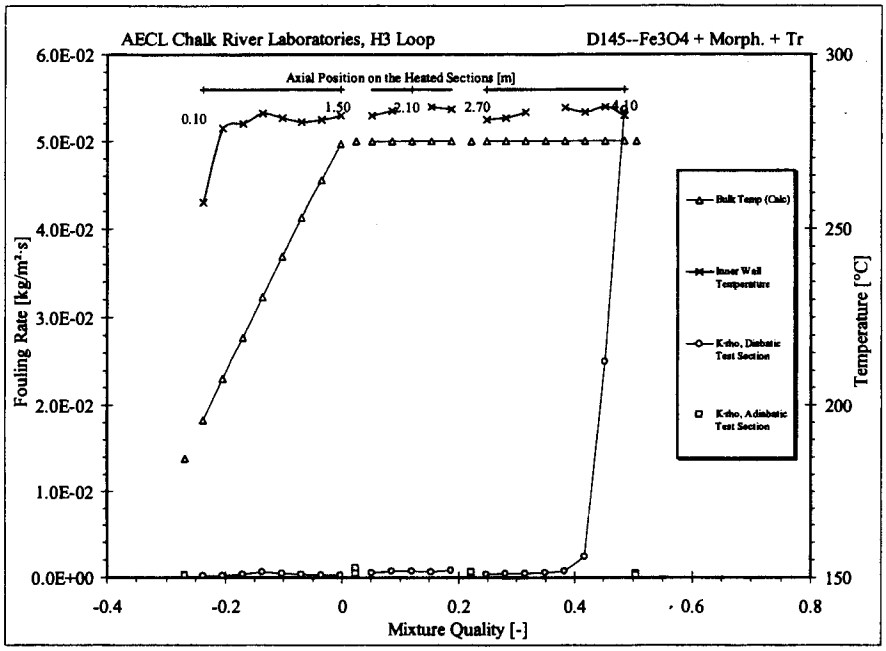

Figure B-7 **Normalized fouling rate versus steam quality. ○ indicates locations along the heated (diabatic) section, □ indicates locations on the unheated (adiabatic) sections.**

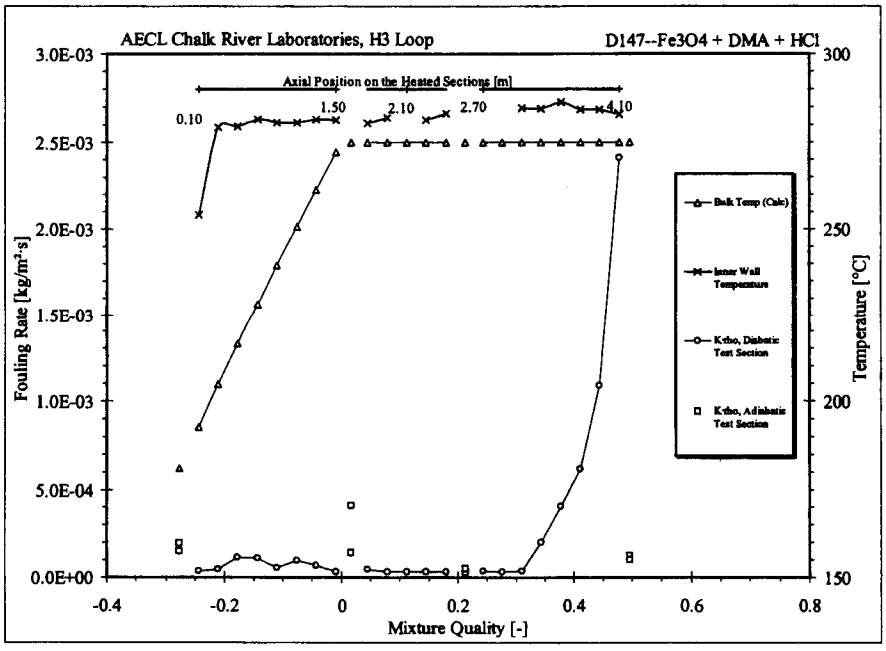

Figure B-8 **Normalized fouling rate versus steam quality. ○ indicates locations along the heated (diabatic) section, □ indicates locations on the unheated (adiabatic) sections.**

DISTRIBUTION

CRL

G.R. Burton, Stn. 80
D. Guzonas, Stn. 61
J. Pietralik, E5
R.L. Tapping, Stn. 80
G. Strati, Stn. 80
E.D. Beaton, Stn. 80

SP

J. Nickerson, SP2F2
N. Subash, SP4F1
Z. Walker, SP2F2

Dominion Engineering
6862 Elm Street
McLean, Virginia 22101

Glenn A. White
Dr. R.D. Varrin

BetzDearborn
P.O. Box 3002
Trevose, PA 19053-6783

Dr. R. Crovetto

Comision Nacional de Energia Atomica
Gerencia de Area Investigaticion y
Desarrollo
Av. Del Libertador 8250
1429 Bs. As.
Argentina

Dr. Mauricio Chocron
Dr. Guillermo Urrutia

Commission Energie Atomic
Centre d'etudes de Cadarache
DEC/SECA/LTEA, Bat 216
St. Paul lez Durance
Cedex 13108
France

Dr. Sylviane Pascal-Ribot
Dr. Delphine Soussan

University of New Brunswick
Nuclear Engineering
Fredericton, New Brunswick
E3B 6C2

Dr. D.H. Lister

University of British Columbia

Dr. P. Watkinson

ISSN 0067-0367

To identify individual documents in the series, we have assigned an AECL-number to each.

Please refer to the AECL-number when requesting additional copies of this document from:

Information Centre, Information Management Branch
AECL
Chalk River, Ontario
Canada K0J 1J0

Fax: (613) 584-8144 Tel.: (613) 584-3311 ext. 4623

Pour identifier les rapports individuels faisant partie de cette series, nous avons affecté un numéro AECL-à chacun d'eux.

Veuillex indiquer le numéro AECL-lorsque vous demandez d'autres exemplaires de ce rapport au:

Service de Distribuition des Documents Officiels
EACL
Chalk River (Ontario)
Canada K0J 1J0

Fax: (613) 584-8144 Tel.: (613) 584-3311 poste 4623